Downloaded on March 5, 2014. The Journal of Clinical Investigation. More information at www.jci.org/articles/view/68964

Serum IgE clearance is facilitated by human FcεRI internalization

Alexandra M. Greer,[1] Nan Wu,[1] Amy L. Putnam,[2] Prescott G. Woodruff,[3] Paul Wolters,[3] Jean-Pierre Kinet,[4] and Jeoung-Sook Shin[1]

[1]Department of Microbiology and Immunology, Sandler Asthma Basic Research Center, [2]Diabetes Center, and [3]Division of Pulmonary, Critical Care, Sleep and Allergy, UCSF, San Francisco, California, USA. [4]Beth Israel Deaconess Medical Center, Harvard University, Boston, Massachusetts, USA.

The high-affinity IgE receptor FcεRI is constitutively expressed in mast cells and basophils and is required for transmitting stimulatory signals upon engagement of IgE-bound allergens. FcεRI is also constitutively expressed in dendritic cells (DCs) and monocytes in humans; however, the specific functions of the FcεRI expressed by these cells are not completely understood. Here, we found that FcεRI expressed by human blood DC antigen 1–positive (BDCA1⁺) DCs and monocytes, but not basophils, traffics to endolysosomal compartments under steady-state conditions. Furthermore, IgE bound to FcεRI on BDCA1⁺ DCs was rapidly endocytosed, transported to the lysosomes, and degraded in vitro. IgE injected into mice expressing human FcεRIα (*FCER1A*-Tg mice) was endocytosed by conventional DCs and monocytes, and endocytosis was associated with rapid clearance of circulating IgE from these mice. Importantly, this rapid IgE clearance was dependent on monocytes or DCs but not basophils. These findings strongly suggest that constitutive internalization of human FcεRI by DCs and monocytes distinctively contributes to serum IgE clearance.

Introduction

FcεRI is the high-affinity IgE receptor best known for its role in mediating allergic reactions. It is assembled from multiple protein subunits: an IgE-binding α subunit; two immunoreceptor tyrosine-based activation motif–containing (ITAM-containing), signal-transducing γ subunits; and an ITAM-containing, signal-amplifying β subunit (1–4). The α subunit associates with the β and/or γ subunits in the ER, which is required for ER exit and subsequent transport to the plasma membranes (5).

FcεRI is highly expressed in mast cells and basophils. When crosslinked by cognate allergens, IgE/FcεRI complexes on these cells initiate a signaling cascade that induces degranulation, which results in the release of inflammatory mediators such as histamine and creates the typical symptoms of acute allergic reaction (4). In humans, but not rodents, FcεRI is expressed not only in basophils and mast cells, but in DCs — including BDCA1⁺ DCs, plasmacytoid DCs, and Langerhans cells — and monocytes in the steady state (6–8). In cases of inflammation, such as viral infection, mice express FcεRI in some DCs (9–11). Unlike mast cells and basophils, DCs and monocytes lack FcεRIβ and thus express FcεRI in its trimeric form (αγγ) (12). Previous studies have shown that when crosslinked by multivalent antigens, antigen:IgE:FcεRI complexes are rapidly endocytosed by BDCA1⁺ DCs and monocytes, and the antigens are subsequently presented to T cells (13, 14). This antigen presentation has been suggested to significantly contribute to Th2 inflammation associated with allergic diseases (13–15).

IgE binding to FcεRI has been shown to stabilize FcεRI expression at the cell surface in vitro (16). Consistent with cell surface stabilization, mast cell and basophil FcεRI surface levels increase as serum IgE concentration increases in both humans and mice (8, 17–19). This presumably enhances the ability of mast cells and basophils to sense and react to allergens during allergic responses. However, whether FcεRI on DCs and monocytes is also stabilized by IgE binding is not clearly established. Some studies have shown that surface FcεRI of human blood BDCA1⁺ DCs and monocytes correlates positively with serum IgE levels (20, 21). However, other studies have shown a lack of correlation between IgE levels in blood and FcεRI levels on BDCA1⁺ DCs or monocytes among individuals with normal ranges of serum IgE levels (8, 22). These findings raise the possibility that FcεRI surface expression in DCs and monocytes may be regulated uniquely from mast cells and basophils, and perhaps independently of IgE.

In this study, we compared human blood basophils and BDCA1⁺ DCs for their ability to regulate surface FcεRI expression in response to serum IgE. We also examined FcεRI intracellular trafficking in these cells as well as monocytes, and how FcεRI trafficking influences the fate of IgE. From these and additional studies using human FcεRI-transgenic mice, we reveal that FcεRI expressed in DCs and monocytes distinctively traffics to lysosomes, and uniquely participates in serum IgE clearance.

Results

The surface level of FcεRI is tightly regulated in BDCA1⁺ DCs compared with basophils. We recruited 11 healthy adult blood donors (Supplemental Table 1; supplemental material available online with this article; doi:10.1172/JCI68964DS1) and examined the correlation between serum IgE levels and surface FcεRI levels in basophils and BDCA1⁺ DCs (hereafter referred to as DCs). Serum IgE concentration was determined by ELISA. FcεRI surface levels were determined by flow cytometry using the antibody CRA-1, which binds to FcεRI irrespective of its binding to IgE (Figure 1A). IgE surface levels were also determined by flow cytometry using an anti-IgE antibody (Figure 1A). We found that FcεRI surface levels increased with serum IgE concentration in both basophils and DCs, but to a much lesser degree in DCs; when a line of best fit was calculated for each cell type, the slope for basophils was more than an order of magnitude greater than the slope for DCs (Figure 1B). The same trend was seen with surface IgE levels, which rose rapidly in basophils with serum IgE but much slower in DCs (Figure 1C). Thus,

Conflict of interest: The authors have declared that no conflict of interest exists.
Citation for this article: *J Clin Invest.* 2014;124(3):1187–1198. doi:10.1172/JCI68964.

Downloaded on March 5, 2014. The Journal of Clinical Investigation. More information at www.jci.org/articles/view/68964

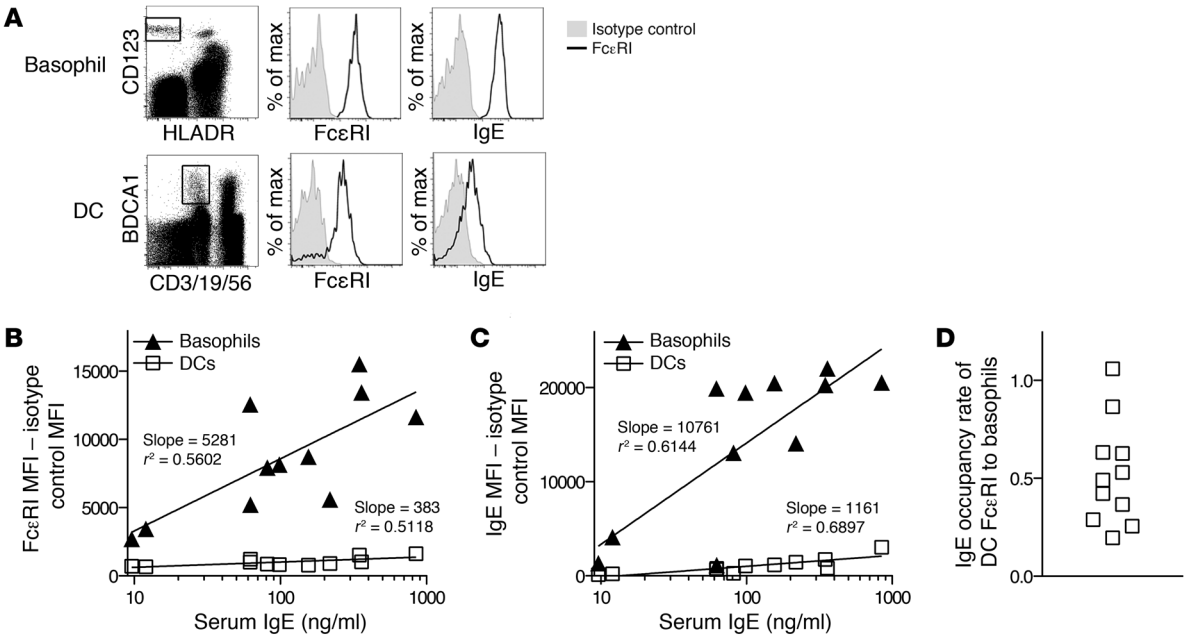

Figure 1

DCs regulate FcεRI surface expression more tightly than basophils. (**A**) Gating strategy of human basophils and DCs, and histograms of surface FcεRI expression and surface IgE bound to the cells. Anti-hFcεRIα antibody (CRA-1) and anti-hIgE staining are shown in black, and isotype control antibody staining is shown in grey. (**B**) Surface FcεRI levels of human blood basophils and DCs in healthy donors. PBMCs were analyzed for FcεRI expression by flow cytometry, and serum was analyzed for IgE concentration by ELISA. Isotype control stain MFI was subtracted from anti-hFcεRIα antibody stain MFI. Data for each donor were plotted according to serum IgE level. Lines of best fit were calculated and drawn; slope and r^2 values are shown. (**C**) Surface IgE levels for the same donors as in **B** with similarly calculated lines of fit. (**D**) IgE occupancy rate of FcεRI in DCs as compared with basophils. The MFI of IgE was divided by the MFI of FcεRI for DCs and basophils after subtracting appropriate isotype control MFI values to generate an occupancy index. DC occupancy index was divided by basophil occupancy index to generate an occupancy rate of DCs compared with basophils.

surface FcεRI levels in DCs correlated with serum IgE to a much lesser degree than those in basophils, indicating comparatively tight regulation of surface FcεRI in DCs.

Previous studies have shown that DCs lack FcεRIβ (12) and that FcεRIβ promotes FcεRIα transport from the ER to the plasma membranes, thus enhancing FcεRI surface expression (2). Consistent with this idea, we found that DCs had much lower FcεRI surface levels than basophils in every donor examined (Figure 1B). IgE surface levels were also lower in DCs (Figure 1C). Interestingly, however, the degree of difference appeared greater for IgE than for FcεRI (see the histograms in Figure 1A as an example), suggesting that FcεRI on DCs might be occupied by IgE to a lesser degree than that on basophils. To quantitatively assess FcεRI occupancy in DCs relative to that of basophils, we divided the MFI of IgE by the MFI of FcεRI for DCs and basophils from each donor, and normalized the value of DCs to the value of basophils. Remarkably, we found that FcεRI occupancy in DCs was lower than that in basophils in 10 of 11 donors examined (Figure 1D). This was unexpected considering that these cells were exposed to the same IgE pool in the blood and because the IgE-binding portion of FcεRI, the α-chain (23), is present in both cell types. The relatively low occupancy of FcεRI in DCs raised the possibility that FcεRI on the surfaces of these cells may turn over in an active manner irrespective of IgE binding. Alternatively, DCs may turn over in the blood much faster than basophils. We sought to address the former possibility by comparatively examining FcεRI trafficking in DCs and basophils.

FcεRI is specifically localized in endolysosomes of DCs and monocytes but not of basophils. To determine the trafficking patterns of FcεRI, we examined FcεRI localization in blood basophils and DCs by confocal microscopy. In basophils, FcεRIα was localized in mesh-like structures (Figure 2A), whereas in DCs it was localized in vesicular compartments (Figure 2B). The FcεRI⁺ mesh-like structures in basophils were extensively labeled with calnexin, a marker of the ER, but not with Lamp1, a lysosome marker, indicating that basophil FcεRI was specifically localized in the ER (Figure 2A). In contrast, FcεRI⁺ compartments in DCs were labeled by neither calnexin nor TGN46 (a marker of Golgi), but partially labeled with EEA1 (an early endosome marker) and extensively labeled with Lamp1 and HLA-DR (lysosome markers) (Figure 2B), indicating that DC FcεRI is specifically localized in endolysosomal compartments. To further determine FcεRI endolysosomal localization in DCs, we incubated DCs with FITC-conjugated ovalbumin for 30 minutes at 37°C, washed extensively, and incubated for another 30 minutes. This method has been commonly used to label functional endolysosomes (24). We found that the anti-FcεRIα antibody colocalized strongly with FITC (Figure 2B), confirming that FcεRIα is localized in endolysosomes in DCs. To determine whether FcεRI lysosomal localization is restricted to blood DCs or a general feature of DCs regardless of tissue origin, we performed a similar microscopic analysis using BDCA1⁺ DCs isolated from the lungs. FcεRI expression in these lung DCs was confirmed by flow cytometry prior to microscopy (Supplemental Figure 1). Similar to blood DCs, lung DCs localized FcεRI in Lamp1⁺ lysosomes (Figure 2C).

Downloaded on March 5, 2014. The Journal of Clinical Investigation. More information at www.jci.org/articles/view/68964

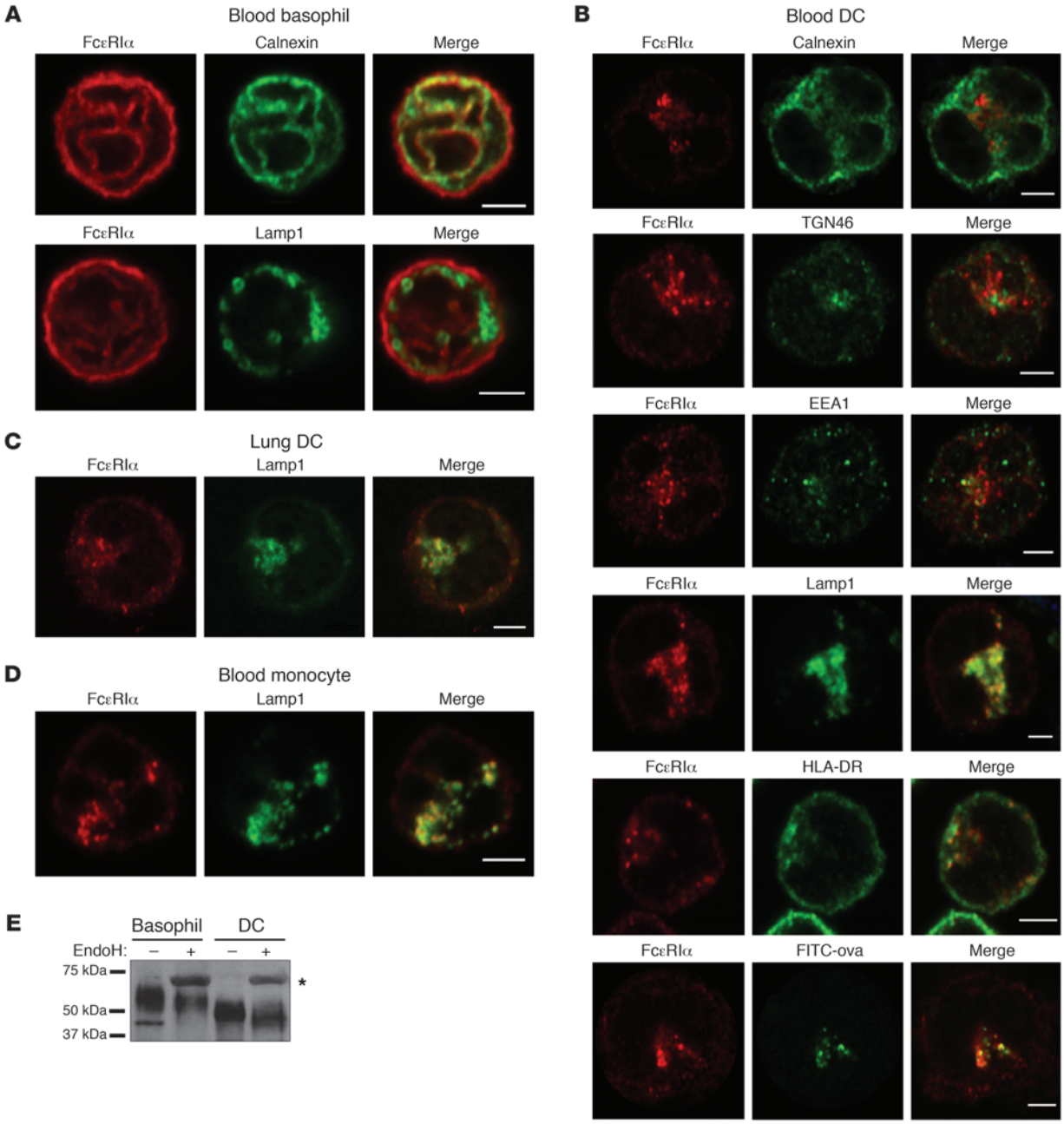

Figure 2

FcεRI is localized in the lysosomes of DCs and monocytes. (**A**–**D**) Intracellular localization of hFcεRI in blood basophils (**A**), blood BDCA1+ DCs (**B**), lung BDCA1+ DCs (**C**), and blood monocytes (**D**). Each cell type was isolated as described in Methods, stained using the indicated antibodies, and examined by confocal microscopy. Basophil images are representative of at least 48 recorded images from at least 7 unique and representative donors. Blood DC images are representative of at least 25 recorded images from 2–6 unique and representative donors. The lung DC image is representative of 10 images from 4 unique and representative donors. The monocyte image is representative of 26 recorded images from 3 unique and representative donors. For all confocal images, original magnification is ×60, scale bars are 2.5 μm, and negligible staining by isotype control antibodies was confirmed (Supplemental Figure 2). (**E**) FcεRIα maturation state in basophils and DCs. FcεRIα was immunoprecipitated from blood basophil and blood BDCA1+ DC lysates. Half of the immunoprecipitates were treated with EndoH. The resulting samples were run on SDS-PAGE, transferred, and blotted with an FcεRIα antibody. The asterisk indicates EndoH that cross-reacted with FcεRIα antisera.

Last, we examined FcεRI localization in monocytes isolated from blood and found that it was also localized in lysosomes labeled by Lamp1 (Figure 2D). These findings indicate that FcεRIα is distinctively localized in endolysosomes in human DCs and monocytes.

FcεRI in DCs is mature. Our confocal microscopy indicated that FcεRIα in basophils is localized in the ER, whereas FcεRIα in DCs and monocytes is mostly excluded from the ER. This finding suggests that a significant portion of FcεRIα is immature in baso-

Downloaded on March 5, 2014. The Journal of Clinical Investigation. More information at www.jci.org/articles/view/68964

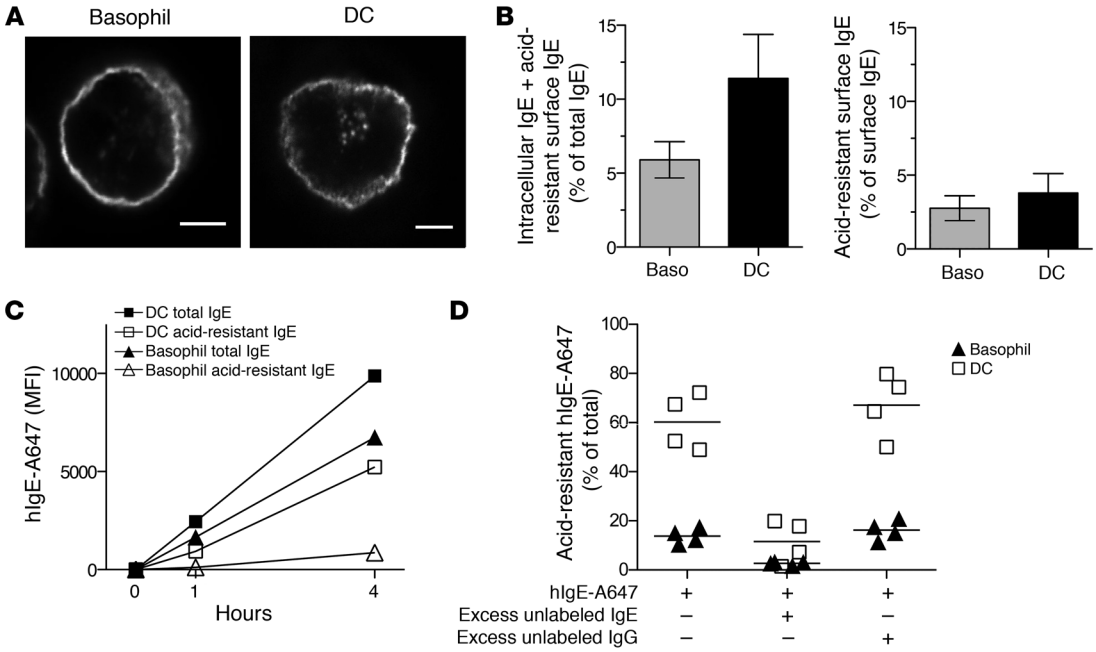

Figure 3

IgE bound to FcεRI on DCs is efficiently internalized. (**A**) Intracellular IgE in basophils and DCs. The basophil image is representative of 83 recorded images from 7 unique and representative donors, and the DC image is representative of 121 recorded images from 9 unique and representative donors. Original magnification, ×60 and scale bars are 2.5 μm. (**B**) Intracellular IgE was quantified by flow cytometry. Isolated basophils and DCs were washed with acid (see Methods for detail) or PBS. Data are mean ± SEM for 8 representative donors. (**C**) Entry of hIgE-A647 into basophils and DCs of one representative donor. hIgE-A647 (0.5 μg/ml) was added to PBMCs. At each indicated time point, cells were treated with acid or PBS before permeabilization and analysis by flow cytometry. (**D**) IgE entry to basophils and DCs is IgE receptor mediated. PBMCs were incubated for 4 hours with hIgE-A647 (0.5 μg/ml) alone (left), with excess unlabeled IgE (middle), or IgG (40 μg/ml) (right). Cells incubated with hIgE-A647 alone were washed with acid or unwashed. Cells incubated together with excess IgE or IgG were all washed with acid. Then, the A647 MFI of acid-washed cells was divided by that of unwashed cells to comparatively determine intracellular IgE content. Data are mean ± SEM for 4 representative donors.

phils, whereas a majority of FcεRIα in DCs is mature. To confirm this, we directly examined the maturation status of FcεRIα in basophils and DCs by determining its sensitivity to endoglycosidase H (EndoH). EndoH cleaves the high-mannose residues that are attached to immature FcεRIα in the ER; mature α-chain has trimmed glycosylated residues that are resistant to EndoH cleavage (25). In FcεRIα immunoprecipitates from basophils, we found a sharp band at 45 kDa and a smear of bands between 50 and 75 kDa (Figure 2E), consistent with a previous report (17). The 45 kDa band completely disappeared after EndoH treatment, reflecting EndoH-sensitive immature FcεRIα, whereas the bands between 50 and 75 kDa were resistant to EndoH, reflecting mature FcεRIα. When the same experiments were performed with DCs, we saw a smear of bands between 40 and 55 kDa, and no extra band was observed. Furthermore, the smear did not disappear after EndoH treatment. This experiment was repeated with cells from another independent donor, and the result was similar (Supplemental Figure 3). This finding suggests that basophils contain both immature and mature FcεRIα, whereas DCs contain FcεRIα mainly in its mature form, with distinct carbohydrate moieties attached.

IgE bound to FcεRI on DCs is efficiently internalized. Our finding that FcεRIα is localized in endolysosomal compartments in DCs raised the possibility that FcεRI might be constitutively endocytosed from the plasma membrane in these cells. In this event, IgE bound to FcεRI at the DC surface would also be endocytosed, and if so, it would be detected inside DCs. To determine the presence of intracellular IgE, we fixed and permeabilized freshly isolated blood basophils and DCs and stained them using an anti-IgE antibody. We found that the anti-IgE antibody mainly labeled the plasma membranes of basophils, while it additionally labeled intracellular compartments in DCs (Figure 3A). To quantitatively determine intracellular IgE, we used flow cytometry to measure the fraction of total IgE left after surface IgE was stripped by an acid wash. We found that approximately 6% of total IgE remained after the stripping of basophils, while approximately 12% was left in DCs (Figure 3B). To examine the possibility that this acid-resistant IgE simply represents surface IgE that was not completely stripped, we determined the efficiency of the acid wash by measuring the fraction of surface IgE remaining after acid treatment. We found that approximately 3% and 4% of surface IgE was not stripped in basophils and DCs, respectively (Figure 3B), indicating that the acid wash could not completely remove surface IgE. Nevertheless, the acid-resistant fraction of total IgE was substantially greater than the acid-resistant fraction of surface IgE in both basophils and DCs (Figure 3B), indicating that both cell types have intracellular IgE, although DCs have significantly more.

To more directly compare the ability of FcεRI on DCs and basophils to mediate IgE internalization, we incubated PBMCs with human IgE conjugated to the fluorophore Alexa Fluor 647 at 37°C for 1 or 4 hours. At each time point, the level of total and acid-resis-

Downloaded on March 5, 2014. The Journal of Clinical Investigation. More information at www.jci.org/articles/view/68964

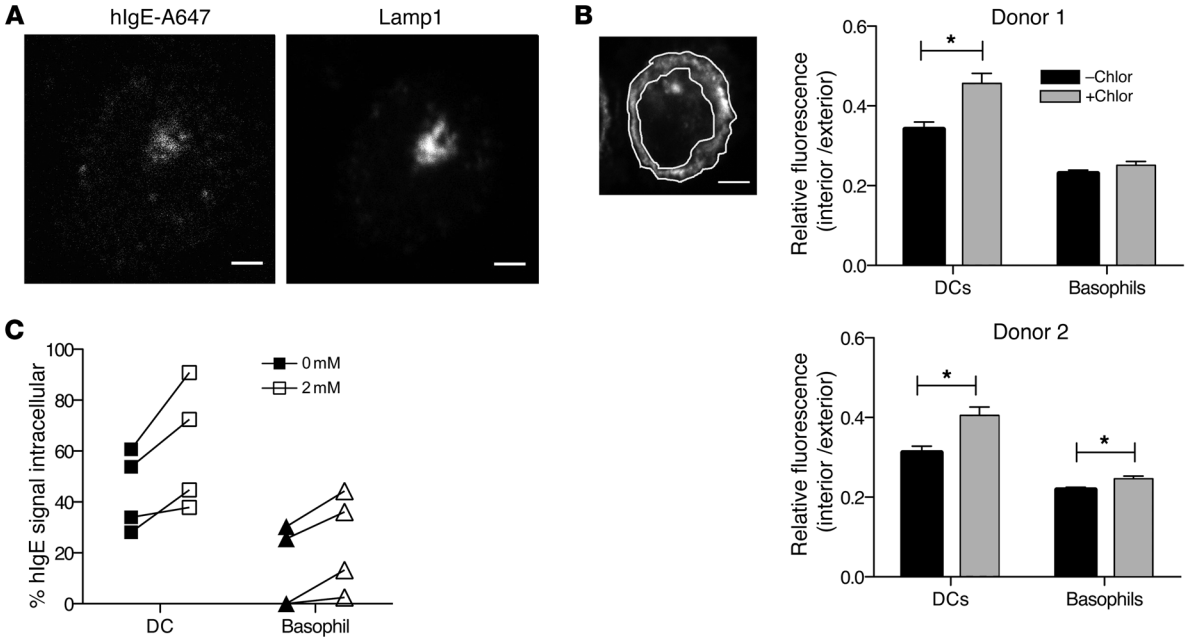

Figure 4

IgE internalized by DCs is delivered to the lysosomes and degraded. (**A**) IgE traffics to lysosomes after entering DCs. DCs were incubated with 0.5 μg/ml hIgE-A647 for 4 hours before preparation for confocal microscopy. Data are representative of 17 images from two unique and representative donors. Original magnification, ×60; scale bars: 2.5 μm. (**B**) Effect of chloroquine on the intracellular IgE pool determined by confocal microscopy. DCs and basophils were incubated for 8 hours at 37°C with or without 0.5 μM chloroquine (Chlor) and stained with anti-IgE antibody before confocal microscopy. On each confocal micrograph, intracellular and cell membrane (extracellular) regions were identified manually (shown on the left; scale bar: 2.5 μm), fluorescence density was measured, and the signal ratio of intracellular to extracellular regions was determined. Shown are summarized data from 30 cells of each type in each condition for 2 donors. Data represent mean ± SEM and $^*P < 0.005$. (**C**) Effect of chloroquine on intracellular IgE pool determined by flow cytometry. Basophils and DCs were incubated for 8 hours at 37°C with or without 2 mM chloroquine and washed with acid or PBS. The acid-resistant IgE fraction was determined by staining cells with anti-IgE after permeabilization and dividing the MFI of acid-washed cells by the MFI of unwashed cells as described for Figure 3B. Data are from 4 representative donors.

tant hIgE–Alexa Fluor 647 associated with DCs and basophils were determined by flow cytometry. We found that total IgE increased over time in both DCs and basophils (Figure 3C and Supplemental Figure 4). Remarkably, the amounts of IgE associated with DCs were comparable to or greater than those associated with basophils (Figure 3C and Supplemental Figure 4), despite FcεRI surface expression being much lower in DCs (Figure 1B), which is consistent with our earlier observation that FcεRI is less occupied by IgE in DCs than in basophils (Figure 1D). We found that acid-resistant IgE also increased over time in both cell types, but to a much higher level in DCs (Figure 3C and Supplemental Figure 4). In fact, up to 60% of total IgE in DCs was acid resistant at 4 hours of incubation, while a maximum of 10% was acid-resistant in basophils (Figure 3D), indicating that DCs internalize IgE more efficiently than basophils do. To verify that internalization is mediated by FcεRI, we performed the same experiment in the presence of excess amounts of unlabeled IgE or IgG. Unlabeled IgE but not IgG markedly inhibited entry of hIgE–Alexa Fluor 647 into both DCs and basophils (Figure 3D), indicating that the entry was indeed IgE receptor mediated. Since the low-affinity IgE receptor FcεRII is not expressed in blood DCs or basophils in the steady state (26, 27), it is FcεRI that mediates internalization of IgE in these cells.

IgE internalized by DCs is delivered to the lysosomes and degraded. Next, we determined the fate of the internalized IgE in DCs and basophils. First, we identified the subcellular localization of hIgE–Alexa Fluor 647 that had entered DCs or basophils by confocal microscopy. While IgE is readily denatured at a pH of 5 and below (28), Alexa Fluor 647 is stable and fluorescent in acidic environments such as lysosomes. We found that Alexa Fluor 647 colocalized with Lamp1 in DCs (Figure 4A), which indicates that IgE had been delivered to the lysosomes. No Alexa Fluor 647 was detected inside basophils (data not shown), consistent with limited entry of IgE into these cells. Second, we determined whether IgE internalized by DCs was degraded in the lysosomes. DCs were isolated from PBMCs and cultured in the presence or absence of chloroquine, an inhibitor of lysosomal acidification (29). After 8 hours of culture, cells were fixed, stained using anti-IgE antibody, and examined by microscopy. We found that chloroquine treatment enlarged the size of the anti-IgE–labeled intracellular compartments specifically in DCs (Supplemental Figure 5). To quantitatively determine the effect of chloroquine on the intracellular IgE pool, we imaged chloroquine-treated and untreated DCs and basophils by confocal microscopy. On the micrographs of each individual cells imaged, the regions of plasma membrane and cytosol were manually drawn (Figure 4B). The anti-IgE antibody signal density in each region was quantitated, and the ratio of cytosolic ("intracellular") to plasma membrane region ("extracellular") signal density was determined. We found that this ratio was significantly higher in chloroquine-treated DCs compared with untreated cells (Figure 4B), indicating that chloroquine treatment increased intracellular

Downloaded on March 5, 2014. The Journal of Clinical Investigation. More information at www.jci.org/articles/view/68964

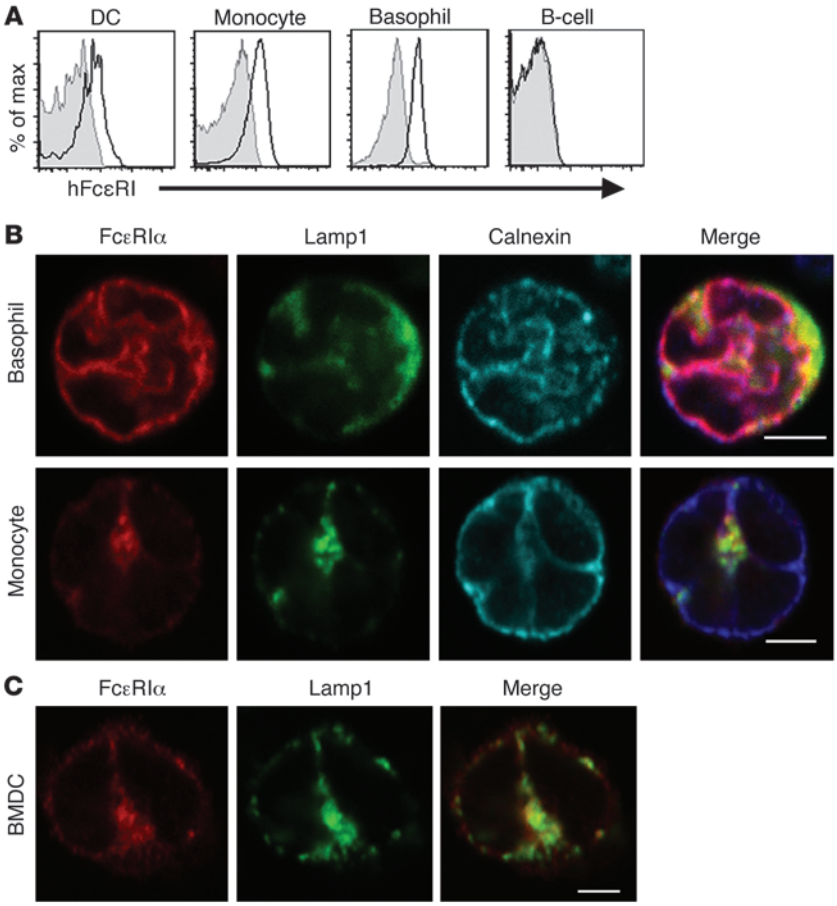

Figure 5

FCER1A-Tg mice express and localize hFcεRI in a similar manner to humans. (**A**) Surface expression of hFcεRI in *FCER1A*-Tg mouse blood leukocytes. Blood from adult hFcεRIα(+) transgenic (Tg$^+$, black) and hFcεRIα(–) (Tg$^-$, gray shaded) littermates was collected and stained with an anti-hFcεRIα antibody and cell type–specific antibodies after red blood cell lysis. Gating strategies are shown in Supplemental Figure 6A. (**B**) Intracellular localization of hFcεRI in Tg$^+$ mouse blood basophils and monocytes. Sorted blood basophils and monocytes were stained for confocal microscopy as described for Figure 2. Images are representative of results from 3 independent experiments. Note that the calnexin signal has been switched from blue to cyan for ease of visualization in single-stain format, while it has not been altered for merged images. (**C**) Intracellular localization of hFcεRI in Tg$^+$ mouse CD11b$^+$ BMDCs. BMDCs were cultured using Flt3L, sorted for CD11b$^+$ cDCs as described for Supplemental Figure 6B, and stained as in **B**. Images are representative results from 3 independent experiments. For all confocal images, magnification was ×60, scale bars are 2.5 μm, and negligible staining by isotype control antibodies was confirmed (Supplemental Figure 7).

IgE in DCs. For comparison, the same experiment was performed using basophils isolated from the same donors. We found that chloroquine treatment did not increase or only slightly increased the intracellular IgE fraction (Figure 4B). Last, we employed flow cytometry to better quantitate the effect of chloroquine on the amount of intracellular IgE. We found that chloroquine treatment consistently increased the fraction of intracellular IgE in DCs (Figure 4C). Notably, intracellular IgE in basophils also increased (Figure 4C), indicating that they too contained some IgE in lysosomes, although markedly less than DCs.

Human FcεRIα is specifically localized in the lysosomes of FCER1A-Tg mouse conventional DCs and monocytes. To obtain evidence that IgE entered DCs via FcεRI in vivo, we used human *FCER1A*-transgenic (*FCER1A*-Tg) mice, which lack mouse *Fcer1a* but express human FcεRIα (*FCER1A*) under transcriptional control of the human promoter (30). We found that these mice expressed hFcεRI on blood conventional DCs (cDCs), monocytes, and basophils, whereas B cells and other lymphocytes did not express it, as in humans (Figure 5A and not shown). hFcεRI in blood basophils of these mice did not colocalize with Lamp1 but did colocalize with calnexin (Figure 5B), similar to observations with human basophils (Figure 2A). We also found that hFcεRIα in blood monocytes of these mice colocalized strongly with Lamp1 (Figure 5B). hFcεRIα in blood cDCs of these mice could not be visualized by microscopy due to the relatively low expression of FcεRIα. Instead, we imaged CD11b$^+$ cDCs (the mouse counterpart of human BDCA1$^+$ DCs; ref. 31) cultured from bone marrow of the mice using Flt3L (ref. 32 and Supplemental Figure 6). hFcεRI in these BMDCs colocalized strongly with Lamp1 (Figure 5C). Thus the cell type–specific expression and trafficking of human FcεRIα was recapitulated in the *FCER1A*-Tg mice.

IgE bound to hFcεRI on monocytes and cDCs is internalized in FCER1A-Tg mice. Having found that, like humans, *FCER1A*-Tg mice express and localize hFcεRI in the lysosomes of cDCs and monocytes, we used these mice to examine whether hFcεRI mediates cellular internalization of IgE in vivo. First, Tg$^+$ and Tg$^-$ mice were i.v. injected with human IgE. It is noteworthy that the injected human IgE had been pre-tested and confirmed for the absence of aggregates that can potentially activate hFcεRI-expressing cells by crosslinking hFcεRI. Briefly, we added the human IgE preparation to mast cells cultured from *FCER1A*-Tg mouse bone marrow and measured degranulation of these cells by a hexosaminidase release assay (33). The addition of up to 10 μg/ml of IgE to the cells did not cause any release of hexosaminidase above the level of spontaneous release (Supplemental Figure 8). In contrast, addition of anti-hFcεRI antibody/secondary antibody complexes resulted in release of 20% of hexosaminidase. These data indicated that the human IgE that we injected to mice did not contain a substantially level of aggregates and would not cause hFcεRI crosslinking in vivo.

After injection of human IgE into Tg$^+$ and Tg$^-$ mice, we bled the mice at multiple time points and determined the amount of human IgE bound to hFcεRI-expressing cells by flow cytometry. We found very little IgE bound to monocytes and basophils of Tg$^-$ mice at all time points examined (Figure 6A). In contrast, surface

Downloaded on March 5, 2014. The Journal of Clinical Investigation. More information at www.jci.org/articles/view/68964

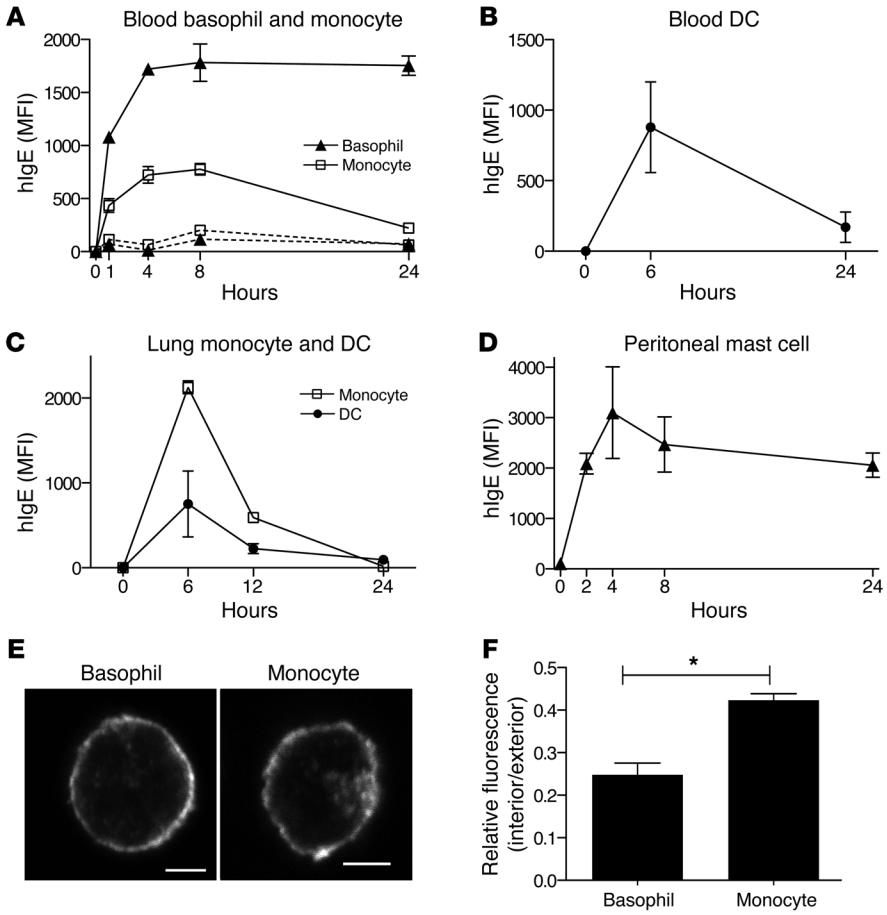

Figure 6

Human IgE injected into *FCER1A*-Tg mice is internalized by cDCs and monocytes in the steady state. (**A**) Surface IgE levels on blood basophils and monocytes following human IgE injection. Before and at 1, 4, 8, and 24 hours after hIgE injection, Tg$^+$ and Tg$^-$ mice were bled for flow cytometric analysis of surface IgE levels in basophils and monocytes. Data for Tg$^+$ mice are shown in solid lines and for Tg$^-$ mice in dotted lines. Data for 3 mice from one representative experiment of 3 are presented with mean ± SEM. (**B**–**D**) Surface IgE levels on blood cDCs (**B**), lung DCs and monocytes (**C**), and peritoneal mast cells (**D**) of Tg$^+$ mice following human IgE injection. At each time point following hIgE injection, mice were sacrificed and whole blood, lungs, or peritoneal lavage collected and analyzed by flow cytometry. Data for 9 mice (**B**), 8 mice (**C**), or 14 mice (**D**) from one representative experiment of 2 are presented with mean ± SEM. (**E** and **F**) Intracellular localization of human IgE in basophils and monocytes of *FCER1A*-Tg mice injected with hIgE. At 6 hours after injection, basophils and monocytes were isolated and examined for intracellular human IgE by confocal microscopy as described for Figure 3A. Original magnification, ×60; scale bars: 2.5 μm. (**F**) Intracellular IgE levels were quantified as in Figure 4B. Thirty images of Tg$^+$ monocytes and basophils were analyzed. Resulting values are presented with mean ± SEM. *$P < 0.05$.

IgE levels increased for both basophils and monocytes in Tg$^+$ mice having reached their maximum approximately 4 hours after injection and remained at least at that level for the next 4 hours (Figure 6A). At 24 hours after injection, however, monocytes had lost approximately 80% of IgE, while basophils retained approximately 100% (Figure 6A). We also monitored IgE on the surface of cDCs in the blood. Since cDCs are scarce in blood, we euthanized individual mice at each time point and performed flow cytometry using whole blood. Similar to monocytes, cDCs lost most of their surface IgE at 24 hours after injection (Figure 6B). In addition to the blood cells, we also examined monocytes and DCs in the lungs. They also captured substantial amounts of IgE but lost most of it as early as 12 hours after injection (Figure 6C). Last, we examined mast cells in the peritoneal cavity. Unlike monocytes and cDCs, these cells retained 100% of the peak surface IgE at 24 hours after injection, similar to basophils (Figure 6D). Notably, hFcεRI was not found in the lysosomes of mast cells but was found on the plasma membranes and ER, as was the case with basophils (Supplemental Figure 9). These findings indicate that human IgE injected into *FCER1A*-Tg mice initially binds to all hFcεRI-expressing cells, but gradually disappears from monocytes and cDCs.

We reasoned that IgE bound to monocytes and cDCs of Tg$^+$ mice could be subsequently internalized, which might explain the gradual loss of IgE from the surface of these cells while the IgE bound to basophils and mast cells remained. Therefore, we looked for intracellular hIgE in blood monocytes and basophils of hIgE-injected Tg$^+$ mice by isolating each cell population at 6 hours after IgE injection, staining with an anti–human IgE antibody after permeabilization, and examining by confocal microscopy. We found that the human IgE was mostly associated with the plasma membranes in basophils, whereas it was detected both at the plasma membranes and in intracellular compartments in monocytes (Figure 6E). Quantification of micrograph images showed that monocytes had a significantly higher proportion of IgE intracellularly compared with basophils (Figure 6F). Taken together, these findings suggest that FcεRI expressed in cDCs and monocytes actively mediates IgE internalization in vivo.

Human FcεRI expressed by cDCs or monocytes contributes to serum IgE clearance in FCER1A-Tg mice. Previous studies have demonstrated that wild-type mice and mFcεRIα-deficient mice clear serum IgE at similar rates, indicating that mFcεRI is not involved in IgE clearance in mice (34, 35). Nevertheless, we hypothesized that human FcεRI could be involved in IgE clearance based on our finding that human FcεRI expressed in monocytes and cDCs mediated cellular internalization of IgE in a constitutive manner. To test this hypothesis, we injected human IgE into Tg$^+$ and Tg$^-$ mice, bled them at various times after injection, and determined serum concentrations of human IgE by ELISA. We found that serum concentrations of human IgE were reduced over time in both strains of mice, but at a markedly accelerated rate in Tg$^+$ mice (Figure 7A). Quantitative analysis showed that the half-life of human IgE in the Tg$^+$ mice was approximately 4-fold shorter than in Tg$^-$ mice (Figure 7B), suggesting that hFcεRI significantly contributes to serum IgE clearance.

Downloaded on March 5, 2014. The Journal of Clinical Investigation. More information at www.jci.org/articles/view/68964

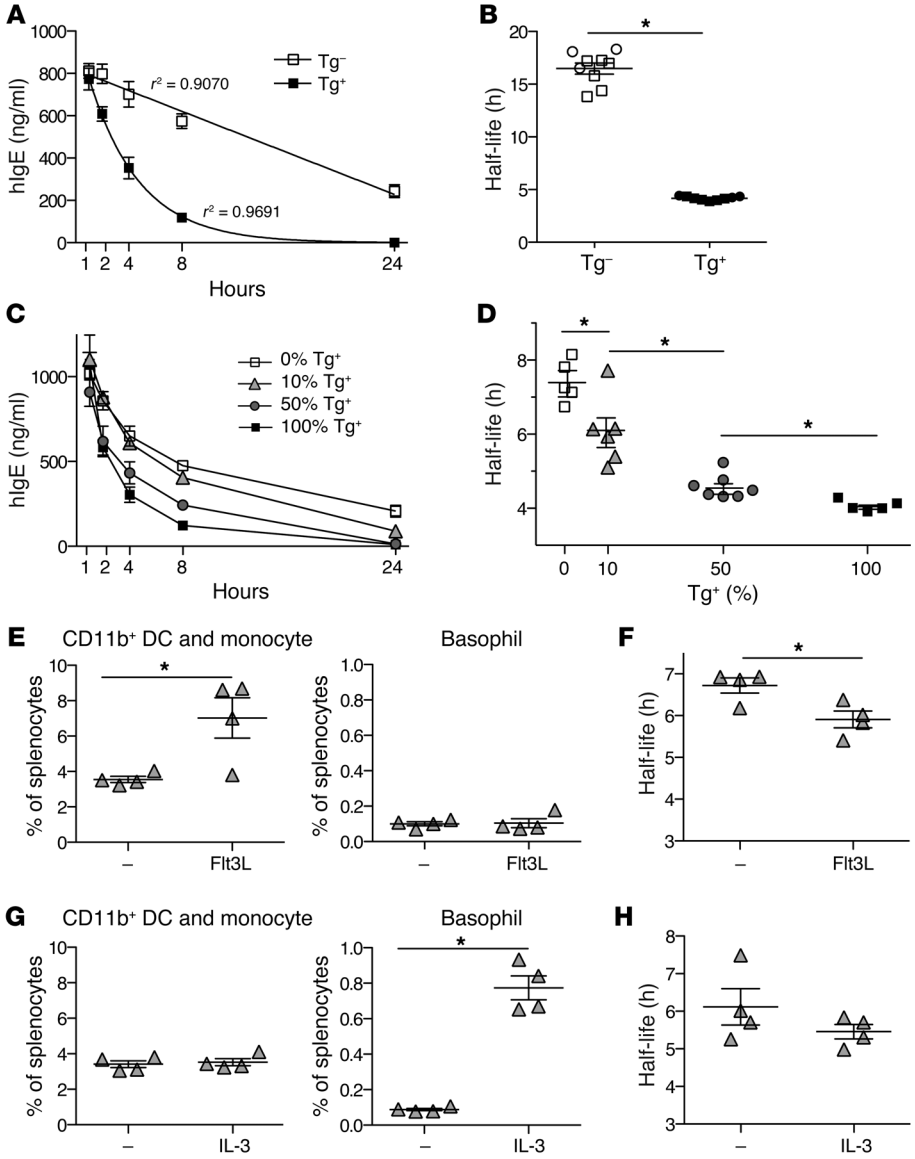

Figure 7

Human FcεRI expressed by DCs or monocytes significantly contributes to serum IgE clearance in *FCER1A*-Tg mice. (**A**) Serum IgE clearance in Tg⁺ and Tg⁻ littermates. 2.5 μg hIgE was i.v. injected into mice, blood was collected following injection, and hIgE concentration was determined by ELISA. Data are representative of 3 independent experiments using 3 mice per strain. For each mean, a line of best fit with indicated r^2 values was calculated. (**B**) Serum half-life of hIgE in Tg⁺ and Tg⁻ mice. IgE half-life was calculated as the time for peak serum IgE to halve from lines of best fit calculated as in **A**. Symbols represent individual mice injected with 2.5 μg (squares) and 5 μg (circles). $^*P < 1.5 \times 10^{-6}$. (**C** and **D**) hFcεRI-expressing hematopoietic cells are responsible for serum IgE clearance. Mixed bone marrow chimeras were made on Tg⁻ recipient hosts, and serum hIgE clearance was examined as described for **A** and **B**. $^*P < 0.05$. (**E** and **G**) Flt3L increases the frequency of DCs/monocytes, while IL-3 increases basophils. 10:90 (Tg⁺/Tg⁻) mixed chimeric mice were injected with Flt3L-expressing B16 cells (**E**) or with IL-3/anti–IL-3 antibody complexes (**G**). The percentage of [CD11b⁺ DCs + monocytes] or basophils in spleen was determined by flow cytometry. $^*P < 0.05$. (**F** and **H**) Serum hIgE clearance is accelerated by an increase in DCs/monocytes but not by an increase in basophils. $^*P < 0.05$. Data in **C**–**H** are representative of 2 independent experiments. The second experiment of **E**–**H** is shown in Supplemental Figure 11.

To verify that the rapid serum IgE clearance observed in Tg⁺ mice is directly attributed to FcεRI-expressing cells and not to some other features associated with genetic alteration of Tg⁺ mice, we reconstituted the hematopoietic compartment of Tg⁻ mice with bone marrow that had been isolated from Tg⁻ or Tg⁺ mice and mixed at specific ratios of Tg⁺ to Tg⁻. We found that mice reconstituted with Tg⁺ bone marrow cleared serum IgE at a much faster rate than those reconstituted with Tg⁻ bone marrow (Figure 7C). We also found that mixed chimeric mice cleared serum IgE in rates proportional to the percentage of Tg⁺ bone marrow used (Figure 7C). Interestingly, however, the half-life of serum IgE in 50% Tg⁺ chimeric mice was comparable to that in 100% Tg⁺ chimeric mice (Figure 7D), suggesting that in this experimental setting, IgE is sufficiently cleared by 50% of the hematopoietic, hFcεRI-expressing cell compartment. Nevertheless, this study demonstrates that it was indeed hFcεRI-expressing cells that were responsible for the rapid serum IgE clearance in *FCER1A*-Tg mice.

Next, we examined the specific contribution of cDCs and monocytes compared with basophils to serum IgE clearance; the former cells internalize and degrade IgE, while the latter retain IgE at the cell surface. Since we found that the rate of IgE clearance increased in proportion to the number of hFcεRI-expressing cells only when these cells were present in limited numbers (Figure 7D), we increased the number of cDCs and monocytes or basophils in 10:90 (Tg⁺/Tg⁻) mixed bone marrow chimeric mice by implanting them with a melanoma cell line producing Flt3L. Flt3L stimulates proliferation and differentiation of the monocyte/DC common progenitor in mice (36, 37). Accordingly, injection of Flt3L or implantation with Flt3L-producing melanoma has been shown to markedly increase the number of monocytes and cDCs in mice (36–38). Consistent with this previous finding, Flt3L melanomas significantly increased the frequency of monocyte and CD11b⁺ cDC, but not basophil, populations (Figure 7E). Note that we did not include CD8⁺ cDCs in this analysis because these DCs expressed hFcεRI at extremely low levels in *FCER1A*-Tg mice (data not shown) and were thus irrelevant to our

Downloaded on March 5, 2014. The Journal of Clinical Investigation. More information at www.jci.org/articles/view/68964

study. Remarkably, Flt3L melanoma–implanted mice cleared serum IgE at a significantly faster rate than untreated mice (Figure 7F). When the same experiment was performed using Tg⁻ mice, however, no difference was observed (Supplemental Figure 10). This finding indicates that neither Flt3L, the melanoma, nor the increase in DCs and monocytes accelerates serum IgE clearance independently of hFcεRI. Next, we increased the frequency of basophils in a separate group of 10:90 (Tg^+/Tg^-) mixed chimeric mice by injecting IL-3/anti–IL-3 antibody complexes. As shown in previous studies (39, 40), this treatment increased the frequency of basophils by approximately 8-fold but did not increase the frequency of monocytes or DCs (Figure 7G). Furthermore, the rate of serum IgE clearance was not accelerated by injection of IL-3/anti–IL-3 antibody complexes (Figure 7H). Taken together, these findings indicate that hFcεRI-expressing cDCs or monocytes, but not basophils, significantly contribute to serum hIgE clearance in *FCER1A*-Tg mice.

Discussion

The present study addressed the question of whether FcεRI expressed in human BDCA1⁺ DCs and monocytes traffics and functions distinctly from that expressed by basophils and mast cells. We found that FcεRI is constitutively endocytosed in these DCs and monocytes, mediating cellular entry of circulating IgE and thus contributing to serum IgE clearance.

Three independent lines of investigation provided evidence that FcεRI is constitutively endocytosed in human BDCA1⁺ DCs and monocytes. First, FcεRI was found in the endocytic compartments of these DCs and monocytes in human blood. It was surprising to find FcεRI in the endolysosomes in cells freshly isolated from blood because previous studies have suggested that FcεRI is endocytosed and transported to the lysosomes only when it is crosslinked by IgE/antigen complexes (13). We find it unlikely that the cells examined had all been engaged by IgE/antigen complexes, because they were isolated from non-allergic healthy blood donors. Furthermore, basophils isolated from the same donors did not show any sign of FcεRI crosslinking such as degranulation; Lamp1, the granular membrane-associated protein, was sequestered intracellularly. In addition, cDCs cultured from the bone marrow of *FCER1A*-Tg mice also localized hFcεRI in the lysosomes. These DCs had not been exposed to any agents capable of interacting with or crosslinking hFcεRI. Thus, FcεRI endolysosomal localization in DCs and monocytes does not seem to be due to FcεRI crosslinking, but attributable to constitutive endolysosomal trafficking of FcεRI in these cells.

Second, BDCA1⁺ DCs in human blood contained an appreciable amount of IgE intracellularly. In addition, fluorescently labeled IgE, when added to these DCs in vitro, was rapidly internalized and delivered to the lysosomes. This internalization was inhibited by excess amounts of unlabeled IgE but not IgG, indicating the internalization was mediated by IgE receptor(s). Since FcεRI is the only IgE receptor DCs express, this finding supports constitutive endocytosis of FcεRI in these cells. Third, hFcεRI expressed in cDCs and monocytes of *FCER1A*-Tg mice was also localized in the lysosomes. Monomeric human IgE injected into these mice was detected at the surface of these cells; however, the IgE soon disappeared from surface but appeared in the intracellular compartments of monocytes. This spontaneous entry of IgE to these cells strongly suggests constitutive endocytosis of FcεRI.

The specific mechanism underlying FcεRI endolysosomal trafficking remains to be determined. We could speculate that FcεRIβ stabilizes FcεRI at the cell surface and that its presence in basophils helps to retain FcεRI at the cell surface, whereas its absence in DCs and monocytes drives FcεRI to the lysosomes. However, genetic ablation of mouse *Fcer1b* in *FCER1A*-Tg mice did not appear to reduce FcεRI surface levels in basophils (3). In addition, the trimeric form of FcεRI (αγγ) expressed in U937 cells was not localized in the lysosomes (data not shown). These data indicate that receptor makeup alone is not sufficient to determine receptor trafficking. Instead, there appear to be cell-intrinsic factors that constitutively mediate FcεRI endocytosis in DCs and monocytes. One potential mechanism is its association with an accessory molecule capable of driving endocytic pathways. The cytoplasmic domain of FcεRI may associate with an adaptor molecule only present in DCs and monocytes that recruits endocytosis protein machineries. Alternatively, FcεRI may interact with an endocytic receptor that facilitates constitutive internalization in cells that express both receptors. For example, DCs and monocytes express many carbohydrate-binding receptors, some of which are constitutively endocytosed (41, 42). One of these may laterally interact with FcεRI through carbohydrate moieties attached to the FcεRIα extracellular domain, thus driving FcεRI to endocytic pathways. Glycosylation of G protein–coupled receptors has been shown to influence the kinetics or routing of endocytosis (43, 44). Notably, FcεRI in BDCA1⁺ DCs appears to be glycosylated distinctly from FcεRI in basophils, as the hFcεRI immunoprecipitated from these DC lysates mobilized, according to SDS-PAGE, at a slightly faster rate.

Previous studies have shown that IgE binding inhibits endocytosis of FcεRI in human basophils and hFcεRI-transfected cell lines, thereby increasing FcεRI surface levels in these cells (45). However, FcεRI surface levels in human blood BDCA1⁺ DCs did not increase with increasing serum IgE as much as those in basophils, suggesting that IgE binding may not stabilize FcεRI on the DC surface. Furthermore, IgE bound to human BDCA1⁺ DCs or bound to hFcεRI-expressing mouse monocytes was rapidly internalized in vitro and in vivo, implicating IgE endocytosis after binding to FcεRI. Thus, the mechanism that mediates FcεRI endocytosis in BDCA1⁺ DCs and monocytes does not appear to be negatively affected by IgE binding.

It is well established that IgE is unique among immunoglobulins in its short serum half-life: it is lost from human serum at a rate 10 times faster than the loss of IgG, resulting in a half-life of roughly 2 days (46, 47). Modeling studies have repeatedly predicted that IgE, distinct from other immunoglobulins, is degraded by two catabolic pathways and that the secondary pathway could involve internalization and degradation of IgE by FcεRI-expressing cells (46). However, this prediction has been largely unsupported by the literature. Mice deficient in FcεRI or mast cells were shown to clear serum IgE as fast as wild-type mice (34, 35, 48). Furthermore, mice with high levels of IgE due to IgE-producing hybridomas also cleared serum IgE at a rate equal to that in normal mice (49), supporting the hypothesis that IgE receptor–bearing cells do not play a significant role in serum IgE loss. While these studies indicate that mouse FcεRI does not significantly contribute to IgE clearance, no studies have examined the role of human FcεRI.

Using *FCER1A*-Tg mice, our studies showed that human FcεRI significantly contributes to serum IgE clearance. By selectively manipulating the number of DCs and monocytes versus basophils in these mice, we further showed that the IgE-clearing role of FcεRI is attributed to its expression in DCs and monocytes,

Downloaded on March 5, 2014. The Journal of Clinical Investigation. More information at www.jci.org/articles/view/68964

but not basophils. Although the underlying mechanisms remain to be determined, the constitutive endocytosis of FcεRI in cDCs and monocytes and consequent entry of IgE into these cells implicates FcεRI-mediated cellular internalization of IgE in serum IgE clearance. It has been shown recently that mouse CD23, the low-affinity IgE receptor, mediates internalization of IgE by B cells but does not contribute to the rate of serum IgE clearance (34). Interestingly, some Fcγ receptors, including FcγRII, -III, and -IV (50, 51), also bind IgE in mice. Therefore, it is plausible that IgG receptors rather than IgE receptors may play a role in clearing IgE in mice.

In summary, we have shown that human FcεRI is constitutively endocytosed and transported to the lysosomes in BDCA1$^+$ DCs and monocytes, and that this mediates cellular entry of circulating IgE and contributes to serum IgE clearance. We speculate that diseases associated with high-serum IgE may involve alteration in FcεRI endolysosomal trafficking in these DCs or monocytes, which would result in an accumulation of IgE in circulation and/or an increase in IgE available to bind to mast cells or basophils. Interestingly, individuals with high IgE — from atopic disease, the genetic disease hyper-IgE syndrome, or IgE myelomas — clear serum IgE at a significantly slower rate than normal individuals (47, 52). Examination of FcεRI trafficking in people with these diseases may reveal new mechanisms of disease pathogenesis, and identification of specific mechanisms directing endocytosis of FcεRI in BDCA1$^+$ DCs and monocytes may lead to novel allergy therapeutics.

Methods

Mice. *FCER1A*-Tg mice have been previously described (30). Neither transgenic nor littermate Tg$^-$ control mice express mFcεRIα. In all experiments, mice were between 4 and 8 weeks old, except bone marrow chimeras, which were 8–12 weeks old. All mice were housed in the UCSF animal facility.

Antibodies. Human IgE was obtained from Abcam and BioFront Technologies and was extensively dialyzed against PBS prior to in vivo experiments. Unlabeled antibodies for confocal microscopy included rabbit polyclonal anti–human/anti–mouse calnexin (Abcam), rabbit polyclonal anti–human TGN46 (Abcam), rabbit polyclonal anti–human EEA1 (Abcam), rabbit polyclonal anti–human HLA-DR (DRAB2, obtained from Yale University, New Haven, Connecticut, USA), mouse monoclonal CRA-1 (anti–human FcεRI α subunit, eBioscience), and goat anti–human IgE (Vector Laboratories). Labeled antibodies for confocal microscopy included Alexa Fluor 488–H4A3 (mouse IgG1 anti–human Lamp1, eBioscience), Alexa Fluor 647–H4A3, and Alexa Fluor 488–1D4B (rat IgG2a anti–mouse Lamp1, BioLegend). Labeled secondary antibodies for confocal microscopy included Invitrogen goat anti–mouse IgG2b–Alexa Fluor 568, goat anti-rabbit Alexa Fluor 647, and rabbit anti-goat Alexa Fluor 568. Labeled anti-human monoclonal antibodies for flow cytometry included BioLegend PerCP/Cy5.5-CD1c (L161, mouse IgG1), Pacific blue–HLA-DR (L243, mouse IgG2a), PE/Cy7-CD14 (HCD14, mouse IgG1) and -CD123 (6H6, mouse IgG1), APC-FcεRIα, PE-FcεRIα (both mouse IgG2b CRA-1), and FITC-CD3 (HIT3A, mouse IgG2a), CD19 (HIB19, mouse IgG1), and CD56 (MEM-188, mouse IgG2a). Labeled anti-mouse antibodies for flow cytometry included BioLegend PE/Cy7-CD11c (N418, Armenian hamster Ig), biotin-CD115 (AFS98, rat IgG2a), PerCP/Cy5.5-CD11b (M1/70, rat IgG2b), Pacific blue–MHC II (M5/114.15.2, rat IgG2b), Alexa Fluor 700–Gr-1 (RB6-8C5, rat IgG2b), FITC-CD49b (DX5, rat IgM), APC–c-kit (ACK2, rat IgG2b), and biotin–anti–human IgE (MHE-18, mouse IgG1). PE-CD131 (rat IgG1) and biotin-CD45RA (14.8, rat IgG2b) were purchased from BD Biosciences. Antibodies for FcεRIα immunoprecipitation and Western blot analysis included a rabbit polyclonal anti-FcεRIα (Upstate) and TrueBlot HRP-conjugated, light chain–specific mouse anti–rabbit IgG (eBioscience). Antibodies for human IgE ELISA included unlabeled G7-18 anti–human IgE (mouse IgG2a, BD Biosciences — Pharmingen), and biotinylated MHE-18 anti-human IgE (mouse IgG1, BioLegend). Rat IgG1 anti–mouse IL-3 antibody (MP2-8F8) for basophil enrichment was purchased from BioLegend.

Blood and lung donors. Blood was collected from reportedly healthy individuals with no history of allergic rhinitis or asthma. Human lung tissues were obtained from lungs originally designated for transplantation by the Northern California Transplant Donor Network but ultimately not used or through lungs resected from patients with lung disease.

Isolation of human DCs, basophils, and monocytes. PBMCs were isolated using Ficoll Plaque Plus (GE Healthcare). BDCA1$^+$ DCs were isolated using the Miltenyi Biotec human DC isolation kit. Non-DCs were saved, and from this, basophils were isolated using the Miltenyi Biotec basophil isolation kit. Cells were checked for purity via flow cytometry; BDCA1$^+$ DCs were 96.4% ± 0.3% SEM pure and were the only FcεRI-expressing cells in the isolates; basophils were approximately 69.8% ± 3.5% SEM pure and were the only FcεRI-expressing cells in the isolates. Monocytes were isolated from PBMCs with the Miltenyi Biotec CD14$^+$ isolation kit, followed by flow cytometric sorting for BDCA1$^-$ cells, yielding extremely pure monocytes (>99%). Lung BDCA1$^+$ DCs were isolated as follows: pieces of lung parenchyma were minced and placed in digestion buffer (HBSS containing 10 mg collagenase D and 2 mg DNase I) for 45 minutes at 37°C while rocking. The generated single-cell suspension was run through Ficoll gradient centrifugation to isolate mononuclear cells. BDCA1$^+$ DCs were isolated from these mononuclear cells using the Miltenyi Biotec human DC isolation kit followed by flow cytometry cell sorting (>99% pure).

Isolation of mouse blood monocytes and basophils, peritoneal mast cells, lung DCs, and CD11b$^+$ BMDCs. To isolate blood monocytes and basophils, PBMCs were isolated from blood with Ficoll Paque Plus. Cells were then stained using an antibody cocktail designed to identify monocytes (CD11b and CD115) and basophils (CD131 and DX5) in 5% BSA/PBS. Each cell type was sorted using a FACSAria3 and FACSDiva (BD) into 50% cold FCS. To isolate peritoneal mast cells, mice were peritoneally lavaged with 3 ml PBS. Lavaged cells were stained using a c-kit antibody, and c-kit$^+$SSC^{hi} cells were sorted by FACS. To isolate lung DCs, mouse lungs were perfused with cold PBS, then excised and digested using the GentleMacs (Miltenyi Biotec) dissociator and digestion buffer (HBSS with 10 mg collagenase D and 2 mg DNase I) and incubated for 30 minutes at 37°C to generate a single-cell suspension. Cells were stained with anti–MHC II and anti-CD11c antibodies, and CD11c$^+$MHC II^{hi} cells were sorted by FACS. To isolate CD11b$^+$ BMDCs, BMDCs were cultured using Flt3L as described previously (32). Cells were stained using anti-CD11c, anti-CD45RA, and anti-CD11b antibodies and CD11c$^+$CD45RA$^-$CD11b$^+$ cells were sorted by flow cytometry.

Generation of bone marrow chimeras. Bone marrow was isolated from femurs and tibias of donor mice, pooled into either Tg$^+$ or Tg$^-$ groups, and placed on ice until injection. Recipient Tg$^-$ mice were irradiated with 550 rad given in 2 doses, 3 hours apart, then reconstituted with 10^7 bone marrow cells within 12 hours of the second irradiation. Mice were housed with antibiotic tablets, and their health was checked daily for 4 weeks following irradiation.

Administration of Flt3L-producing melanoma or IL-3/anti–IL-3 antibody complexes in mice. Murine Flt3L-producing B16 melanoma cells (38) were cultured in DMEM supplemented with 10% FBS, penicillin/streptomycin, and L-glutamine before harvesting for injection. Cells (1×10^6) were injected subcutaneously into the backs of anesthetized mice. Mice were analyzed 14 days after injection. Murine IL-3 was purchased from Peprotech and was stored at 1 μg/μl at –20°C until use. Just before injection, 10 μg IL-3 was thawed and mixed at room temperature with 2 μg of anti–IL-3 antibody for

Downloaded on March 5, 2014. The Journal of Clinical Investigation. More information at www.jci.org/articles/view/68964

1 minute. After 1 minute, the mixture was diluted with PBS to 100 μl total. Mice were anesthetized, injected i.v. with the IL-3/antibody mixture, and analyzed 5 days after injection.

Cell culture. BMDCs were generated by culturing *FCER1A*-Tg mouse bone marrow for 6 days in DMEM media supplemented with 10% FBS, L-glutamine, penicillin/streptomycin, and 100 ng/ml recombinant mouse Flt3L. On day 6, cells were stained and sorted for CD11b$^+$ cells. Bone marrow-derived mast cells (BMMCs) were generated by isolating bone marrow from an *FCER1A*-Tg mouse and culturing the cells for 3 weeks in RPMI media supplemented with 10% FBS, L-glutamine, penicillin/streptomycin, IL-3 (5 ng/ml), and SCF (5 ng/ml). Media and culture flasks were changed every week. Purity of the cells was determined by flow cytometry at the end of 3 weeks in culture; more than 95% of cells were c-kit$^+$hFcεRI$^+$.

Hexosaminidase release assay. The colorimetric hexosaminidase release assay was employed as described previously (33). Briefly, BMMCs equilibrated with Tyroid buffer were mixed with human IgE or anti-hFcεRI antibody:anti–mouse IgG antibody complexes in a 96 well plate. After incubating at 37°C for 1 hour, the plate was centrifuged, supernatant was collected, and cell pellet was lysed with 0.1% Triton X-100. The supernatant and cell lysates were mixed with the hexosaminidase substrate *p*-nitrophenyl-*N*-acetyl-β-D-glucosaminide (1 mM). After incubating at 37°C for 1 hour, 0.1 M sodium acetate buffer was added to stop the enzyme reaction, and absorbance was read at 400 nm.

Confocal microscopy. Single-cell suspensions layered on Alcian blue–treated coverslips were fixed with 4% paraformaldehyde, permeabilized with 0.05% saponin in 10% goat serum or 5% BSA, and stained with specific primary antibodies or isotype control antibodies, followed by fluorophore-conjugated secondary antibodies. Confocal microscopy was performed with a Nikon C1si spectral confocal microscope with a ×60 Plan Apo oil-immersion objective (Nikon) at the Biological Imaging Developmental Center at UCSF or using a Leica SP5 spectral confocal microscope with a ×63 Plan Apo oil-immersion objective (Leica).

Immunoprecipitation and Western blot analysis. 7.5×10^5 human blood basophils and 6.4×10^6 blood BDCA1$^+$ DCs from an anonymous donor were isolated from apheresis tubing. Cells were lysed in 75 and 640 μl of cold lysis buffer containing 1% Triton-X, 10 mM Tris, 100 mM NaCl, 5 mM $MgCl_2$ (pH 7.6) with 20 mM *N*-ethylmaleimide (NEM, Sigma-Aldrich) and protease inhibitor cocktail (Thermo) freshly added. FcεRIα was immunoprecipitated with a rabbit polyclonal anti-FcεRIα antisera (Upstate) and protein G sepharose beads (GE Healthcare). The immunoprecipitates were split into two samples. One sample had sample buffer added and was boiled for 10 minutes, and the other sample was treated with EndoH (New England Biolabs) for 2 hours at 37°C before sample buffer was added. Samples were run on SDS-PAGE, and Western blot analysis was performed using FcεRIα-specific rabbit antisera and HRP-conjugated anti-rabbit antibody.

Quantification of fluorescence intensity from confocal micrographs. Single-cell images from human or mouse were obtained at a distance of 3 μm from the bottom of the cell via confocal microscopy using controlled laser intensity and gain for each cell type. For each image, the intracellular portion and cell membrane (extracellular) were identified, and the MFI/area was determined by using FIJI software (http://fiji.sc/Fiji). For human cells, 30 BDCA1$^+$ DCs and 30 basophils were analyzed and plotted as intracellular/extracellular MFI/area. For mouse cells, intracellular and extracellular IgE MFI was determined from 10 monocytes and 10 basophils from Tg$^-$ mice following IgE injection, and the results were averaged to control for autofluorescence. Then, 30 monocytes and basophils from Tg$^+$ mice injected with IgE were analyzed and corrected for autofluorescence by subtracting the Tg$^-$ averages, then plotted as intracellular/extracellular IgE MFI.

Acid stripping of human DCs and basophils. Human PBMCs were isolated as described above and put into two samples. One sample was incubated with ice-cold acetic acid buffer (0.2 M acetic acid, 0.15 M NaCl, pH 2.5) for 5 minutes on ice, and the other sample was incubated with PBS. After 5 minutes, samples were spun at 250 *g* for 5 minutes without adding any media. After spinning, the supernatant was aspirated, and cells were resuspended in 5% BSA in PBS and spun again. All samples were then fixed and permeabilized using the BD Fixation/Permeabilization kit according to the manufacturer's instructions before staining with antibodies against cell-specific markers and IgE or an isotype control. Parallel samples of non-fixed and non-permeabilized cells were also stripped, stained, and analyzed as controls for the efficiency of acid stripping. To determine the acid-resistant fraction of total IgE, cells were permeabilized and stained with an anti-IgE antibody, and the MFI of acid-washed cells was divided by that of unwashed cells. To determine the acid-resistant fraction of surface IgE, cells were stained with anti-IgE without permeabilization, and the MFI of acid-washed cells was divided by that of unwashed cells.

Flow cytometry. All samples were run using FACSDiva on a BD LSRII cytometer at low or medium speed, and all experiments were analyzed using FlowJo software (Tree Star). For all experiments excluding intracellular staining, live (PI-negative) singlet cells were used for final data analysis.

Human IgE ELISA. For serum IgE ELISA experiments, 2.5 μg of human IgE in 100 μl PBS was injected retro-orbitally into isoflurane-anesthetized mice. Serum at the 0 hour time point was taken at least 1 day before the experiment. At 1, 2, 4, 8, and 24 hours after hIgE injection, a small amount of blood was collected into PCR strip tubes via submandibular bleed, and serum was collected for ELISA. Samples were diluted to 1:40 in 1% BSA for ELISA, and human IgE from the same lot was also diluted for a standard curve. A standard ELISA protocol was used with G7-18 and biotinylated MHE-18 anti-IgE antibodies. Plates were read using an XFluor plate reader (Tecan), and data analysis was performed with Excel (Microsoft) and Prism software (GraphPad).

Statistics. For all experiments, statistical significance was determined via unpaired, 2-tailed *t* tests. *P* values of less than 0.05 were considered significant.

Study approval. All animal experiments and procedures were performed according to protocols approved by the UCSF Institutional Animal Ethics Committee. Human blood donors gave written and informed consent for flow cytometric analysis of blood cells and clinical testing of serum IgE levels. Experiments using human blood and lung samples were performed under UCSF Committee on Human Research–approved protocols 11-07039, 10-02596, and 10-00198.

Acknowledgments

We thank the UCSF Biological Imaging Development Center (BIDC) microscopy core facility, Sophia Majeed, and Frances Brodsky for their support for confocal microscopy. We also thank Aaron Whiteley and Richard Locksley for critical reading of the manuscript. This work was supported by the American Asthma Foundation (to J.-S. Shin), the American Heart Association (10SDG3500062 to J.-S. Shin), the Sandler Asthma Basic Research Center (to J.-S. Shin), NIH T32 AI007334 (to A.M. Greer), and a UCSF fellowship in the Graduate Education in Medical Sciences program (to A.M. Greer).

Received for publication January 23, 2013, and accepted in revised form December 12, 2013.

Address correspondence to: Jeoung-Sook Shin, UCSF Department of Microbiology and Immunology, 513 Parnassus Avenue, Box 0414, San Francisco, California 94143, USA. Phone: 415.476.5451; Fax: 415.476.3939; E-mail: jeoung-sook.shin@ucsf.edu.

Downloaded on March 5, 2014. The Journal of Clinical Investigation. More information at www.jci.org/articles/view/68964

1. Lin S, Cicala C, Scharenberg AM, Kinet JP. The FcεRIβ subunit functions as an amplifier of FcεRIγ-mediated cell activation signals. *Cell*. 1996; 85(7):985–995.
2. Donnadieu E, Jouvin MH, Kinet JP. A second amplifier function for the allergy-associated FcεRIβ subunit. *Immunity*. 2000;12(5):515–523.
3. Dombrowicz D, et al. Allergy-associated FcRβ is a molecular amplifier of IgE- and IgG-mediated in vivo responses. *Immunity*. 1998;8(4):517–529.
4. Gould HJ, Sutton BJ. IgE in allergy and asthma today. *Nat Rev Immunol*. 2008;8(3):205–217.
5. Letourneur F, Hennecke S, Démollière C, Cosson P. Steric masking of a dilysine endoplasmic reticulum retention motif during assembly of the human high affinity receptor for immunoglobulin E. *J Cell Biol*. 1995;129(4):971–978.
6. Maurer D, et al. Expression of functional high affinity immunoglobulin E receptors (FcεRI) on monocytes of atopic individuals. *J Exp Med*. 1994; 179(2):745–750.
7. Takenaka M, Tanaka Y, Anan S, Yoshida H, Ra C. High affinity IgE receptor-mediated prostaglandin E2 production by monocytes in atopic dermatitis. *Int Arch Allergy Immunol*. 1995;108(3):247–253.
8. Foster B, Metcalfe DD, Prussin C. Human dendritic cell 1 and dendritic cell 2 subsets express FcεRI: correlation with serum IgE and allergic asthma. *J Allergy Clin Immunol*. 2003;112(6):1132–1138.
9. Grayson MH, et al. Induction of high-affinity IgE receptor on lung dendritic cells during viral infection leads to mucous cell metaplasia. *J Exp Med*. 2007;204(11):2759–2769.
10. Hammad H, et al. Inflammatory dendritic cells — not basophils — are necessary and sufficient for induction of Th2 immunity to inhaled house dust mite allergen. *J Exp Med*. 2010;207(10):2097–2111.
11. Plantinga M, et al. Conventional and monocyte-derived CD11b(+) dendritic cells initiate and maintain T helper 2 cell-mediated immunity to house dust mite allergen. *Immunity*. 2013;38(2):322–335.
12. Maurer D, et al. Peripheral blood dendritic cells express FcεRI as a complex composed of FcεRI α- and FcεRI γ-chains and can use this receptor for IgE-mediated allergen presentation. *J Immunol*. 1996;157(2):607–616.
13. Maurer D, et al. Fc epsilon receptor I on dendritic cells delivers IgE-bound multivalent antigens into a cathepsin S-dependent pathway of MHC class II presentation. *J Immunol*. 1998;161(6):2731–2739.
14. Maurer D, et al. The high affinity IgE receptor (FcεRI) mediates IgE-dependent allergen presentation. *J Immunol*. 1995;154(12):6285–6290.
15. Sallmann E, et al. High-affinity IgE receptors on dendritic cells exacerbate Th2-dependent inflammation. *J Immunol*. 2011;187(1):164–171.
16. Borkowski TA, Jouvin MH, Lin SY, Kinet JP. Minimal requirements for IgE-mediated regulation of surface FcεRI. *J Immunol*. 2001;167(3):1290–1296.
17. Saini SS, et al. Expression and modulation of FcεRIα and FcεRIβ in human blood basophils. *J Allergy Clin Immunol*. 2001;107(5):832–841.
18. Yamaguchi M, et al. IgE enhances mouse mast cell FcεRI expression in vitro and in vivo: evidence for a novel amplification mechanism in IgE-dependent reactions. *J Exp Med*. 1997;185(4):663–672.
19. Conroy MC, Adkinson NF, lichtenstein LM. Measurement of IgE on human basophils: relation to serum IgE and anti-IgE-induced histamine release. *J Immunol*. 1977;118(4):1317–1321.
20. Vasudev M, et al. Expression of high-affinity IgE receptor on human peripheral blood dendritic cells in children. *PLoS One*. 2012;7(2):e32556.
21. Sihra BS, Kon OM, Grant JA, Kay AB. Expression of high-affinity IgE receptors (FcεRI) on peripheral blood basophils, monocytes, and eosinophils in atopic and nonatopic subjects: relationship to total serum IgE concentrations. *J Allergy Clin Immunol*. 1997;99(5):699–706.
22. Dehlink E, Baker AH, Yen E, Nurko S, Fiebiger E. Relationships between levels of serum IgE, cell-bound IgE, and IgE-receptors on peripheral blood cells in a pediatric population. *PLoS One*. 2010;5(8):e12204.
23. Hakimi J, et al. The alpha subunit of the human IgE receptor (FcERI) is sufficient for high affinity IgE binding. *J Biol Chem*. 1990;265(36):22079–22081.
24. Garrett WS, et al. Developmental control of endocytosis in dendritic cells by Cdc42. *Cell*. 2000; 102(3):325–334.
25. Albrecht B, Woisetschläger M, Robertson MW. Export of the high affinity IgE receptor from the endoplasmic reticulum depends on a glycosylation-mediated quality control mechanism. *J Immunol*. 2000;165(10):5686–5694.
26. Krauss S, Mayer E, Rank G, Rieber EP. Induction of the low affinity receptor for IgE (FcεRII/CD23) on human blood dendritic cells by interleukin-4. *Adv Exp Med Biol*. 1993;329:231–236.
27. MacGlashan D, et al. Upregulation of FcεRI on human basophils by IgE antibody is mediated by interaction of IgE with FcεRI. *J Allergy Clin Immunol*. 1999;104(2 pt 1):492–498.
28. Demarest SJ, et al. An intermediate pH unfolding transition abrogates the ability of IgE to interact with its high affinity receptor FcεRIα. *J Biol Chem*. 2006;281(41):30755–30767.
29. Mellman I, Fuchs R, Helenius A. Acidification of the endocytic and exocytic pathways. *Annu Rev Biochem*. 1986;55:663–700.
30. Dombrowicz D, et al. Anaphylaxis mediated through a humanized high affinity IgE receptor. *J Immunol*. 1996;157(4):1645–1651.
31. Robbins SH, et al. Novel insights into the relationships between dendritic cell subsets in human and mouse revealed by genome-wide expression profiling. *Genome Biol*. 2008;9(1):R17.
32. Naik SH, et al. Cutting edge: generation of splenic CD8+ and CD8- dendritic cell equivalents in Fms-like tyrosine kinase 3 ligand bone marrow cultures. *J Immunol*. 2005;174(11):6592–6597.
33. Shin J-S, Shelburne CP, Jin C, LeFurgey EA, Abraham SN. Harboring of particulate allergens within secretory compartments by mast cells following IgE/FεRI-lipid raft-mediated phagocytosis. *J Immunol*. 2006;177(9):5791–5800.
34. Cheng LE, Wang Z-E, Locksley RM. Murine B cells regulate serum IgE levels in a CD23-dependent manner. *J Immunol*. 2010;185(9):5040–5047.
35. Dombrowicz D, Flamand V, Brigman KK, Koller BH, Kinet JP. Abolition of anaphylaxis by targeted disruption of the high affinity immunoglobulin E receptor α chain gene. *Cell*. 1993;75(5):969–976.
36. Waskow C, et al. The receptor tyrosine kinase Flt3 is required for dendritic cell development in peripheral lymphoid tissues. *Nat Immunol*. 2008;9(6):676–683.
37. Liu K, et al. In vivo analysis of dendritic cell development and homeostasis. *Science*. 2009; 324(5925):392–397.
38. Mach N, et al. Differences in dendritic cells stimulated in vivo by tumors engineered to secrete granulocyte-macrophage colony-stimulating factor or Flt3-ligand. *Cancer Res*. 2000;60(12):3239–3246.
39. Ohmori K, et al. IL-3 induces basophil expansion in vivo by directing granulocyte-monocyte progenitors to differentiate into basophil lineage-restricted progenitors in the bone marrow and by increasing the number of basophil/mast cell progenitors in the spleen. *J Immunol*. 2009;182(5):2835–2841.
40. Finkelman FD, et al. Anti-cytokine antibodies as carrier proteins. Prolongation of in vivo effects of exogenous cytokines by injection of cytokine-anti-cytokine antibody complexes. *J Immunol*. 1993; 151(3):1235–1244.
41. Mahnke K, et al. The dendritic cell receptor for endocytosis, DEC-205, can recycle and enhance antigen presentation via major histocompatibility complex class II-positive lysosomal compartments. *J Cell Biol*. 2000;151(3):673–684.
42. Higashi N, et al. The macrophage C-type lectin specific for galactose/N-acetylgalactosamine is an endocytic receptor expressed on monocyte-derived immature dendritic cells. *J Biol Chem*. 2002; 277(23):20686–20693.
43. Tansky MF, Pothoulakis C, Leeman SE. Functional consequences of alteration of N-linked glycosylation sites on the neurokinin 1 receptor. *Proc Natl Acad Sci USA*. 2007;104(25):10691–10696.
44. Cho DI, et al. The N-terminal region of the dopamine D2 receptor, a rhodopsin-like GPCR, regulates correct integration into the plasma membrane and endocytic routes. *Br J Pharmacol*. 2012;166(2):659–675.
45. MacGlashan D, Xia HZ, Schwartz LB, Gong J. IgE-regulated loss, not IgE-regulated synthesis, controls expression of FcεRI in human basophils. *J Leukoc Biol*. 2001;70(2):207–218.
46. Iio A, Waldmann TA, Strober W. Metabolic study of human IgE: evidence for an extravascular catabolic pathway. *J Immunol*. 1978;120(5):1696–1701.
47. Dreskin SC, Goldsmith PK, Strober W, Zech LA, Gallin JI. Metabolism of immunoglobulin E in patients with markedly elevated serum immunoglobulin E levels. *J Clin Invest*. 1987;79(6):1764–1772.
48. Watanabe N, Owhashi M, Nawa Y. Clearance of passively transferred IgE antibody from peripheral blood of mast cell-deficient W/Wv mice. *Int Arch Allergy Appl Immunol*. 1986;81(4):385–387.
49. Haba S, Ovary Z, Nisonoff A. Clearance of IgE from serum of normal and hybridoma-bearing mice. *J Immunol*. 1985;134(5):3291–3297.
50. Mancardi DA, et al. FcγRIV is a mouse IgE receptor that resembles macrophage FcεRI in humans and promotes IgE-induced lung inflammation. *J Clin Invest*. 2008;118(11):3738–3750.
51. Takizawa F, Adamczewski M, Kinet JP. Identification of the low affinity receptor for immunoglobulin E on mouse mast cells and macrophages as FcγRII and FcγRIII. *J Exp Med*. 1992;176(2):469–475.
52. Waldmann TA, Iio A, Ogawa M, McIntyre OR, Strober W. The metabolism of IgE. Studies in normal individuals and in a patient with IgE myeloma. *J Immunol*. 1976;117(4):1139–1144.

Subjects (n)		11
Age, mean ±SD		29.55 ±3.47
Gender		
	Male, n (%)	7 (64)
	Female, n (%)	4 (36)
Race (n)		
	Caucasian	6
	Asian	5

Supplemental Table 1: Human blood donors.

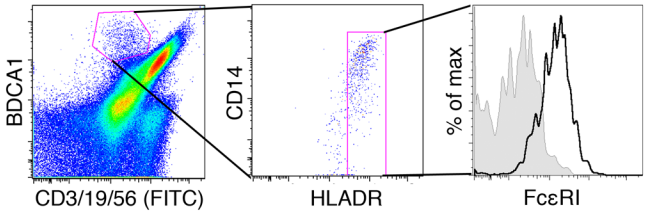

Supplemental Figure 1: Expression of FcεRI in human lung BDCA1+ DCs. Live, singlet cells were stained with a cocktail of antibodies. BDCA1+ DCs were gated by selecting BDCA1+[CD3/19/56]- cells, then further selecting HLADR+ cells. BDCA1+ DCs are FcεRI+, as shown in the histogram on the right. Anti-hFcεRIα antibody (CRA-1) is black, and isotype control is shown in grey. Data shown are from one representative donor of 4 tested.

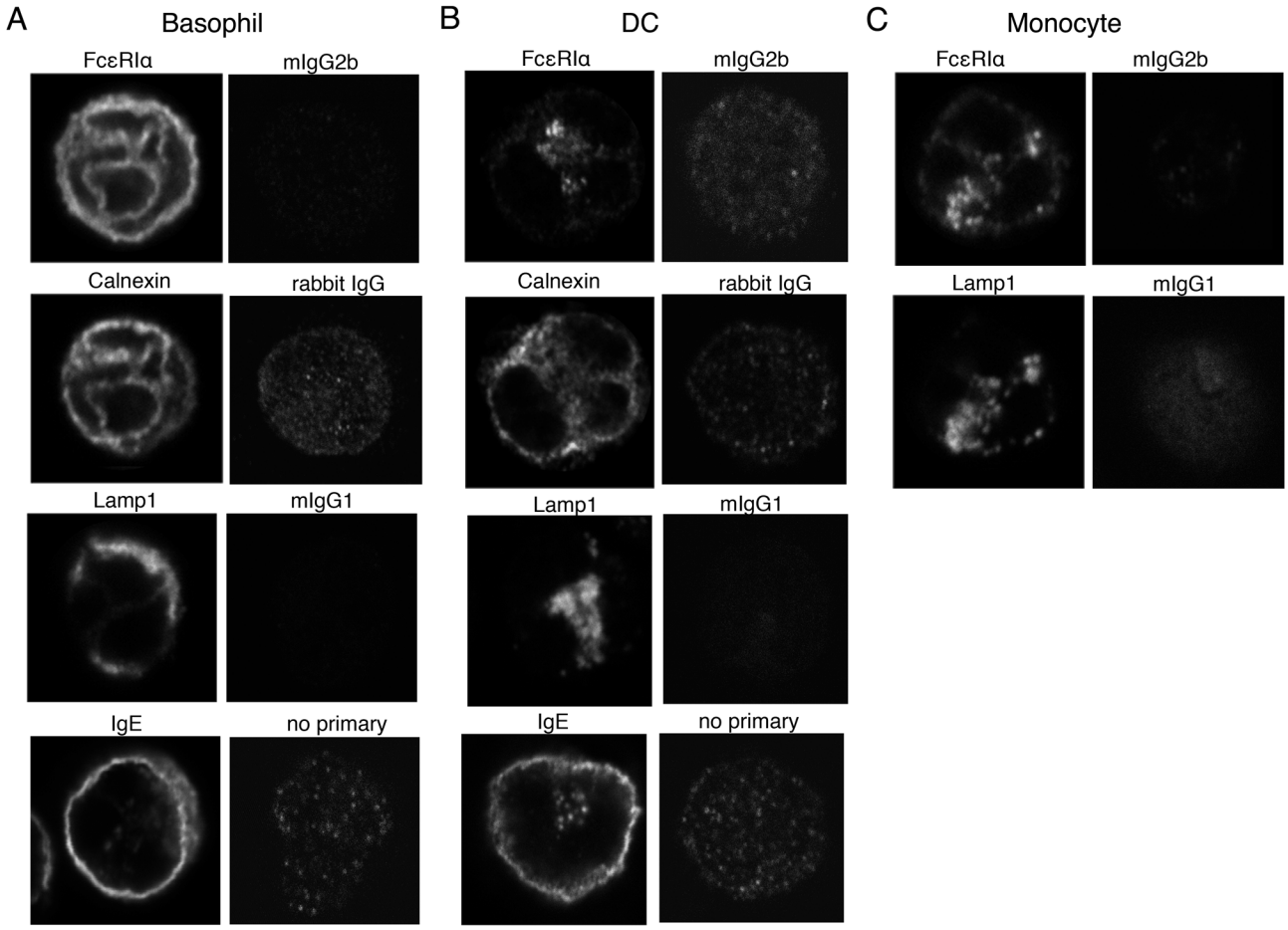

Supplemental Figure 2: Isotype control stains for confocal microscopy of human cells. Basophils **(A)**, DCs **(B)**, and monocytes **(C)** were isolated as per Methods and were stained with antibodies indicated (left panels) or matched isotype control antibodies (right panels). Note that for basophils and DCs, a 'no primary' antibody control was used for IgE.

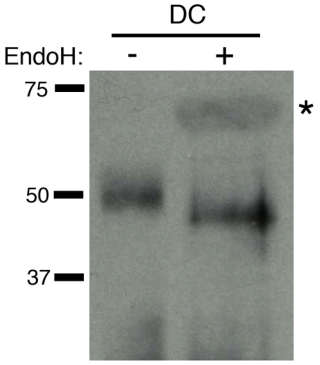

Supplemental Figure 3: Second representative Western blot of FcεRIα. DCs were isolated according to methods and some immunoprecipitated FcεRIα was treated with EndoH.The star indicates EndoH band which cross-reacts with FcεRIα antibody.

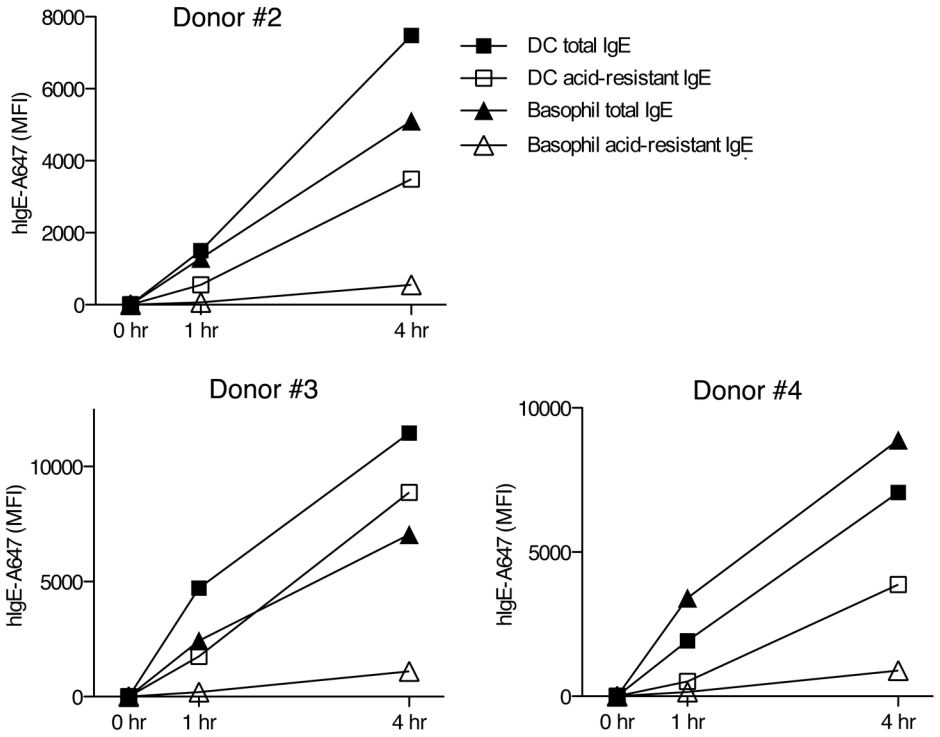

Supplemental Figure 4: hIgE-A647 binding and internalization by DCs and basophils of three additional healthy blood donors. Experiments were run in parallel with that shown in Figure 3C.

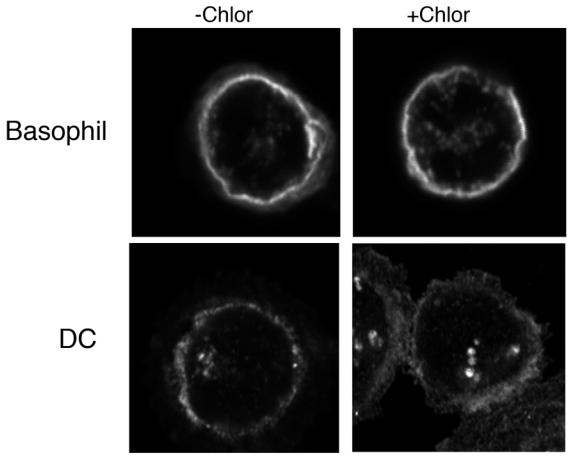

Supplemental Figure 5: The effect of chloroquine on IgE-containing intracellular compartments. Basophils and DCs were incubated for 8 hrs at 37° C with or without 0.5 µM chloroquine (Chlor) and stained with anti-IgE antibody for confocal microscopy. The same laser intensity was employed for chloroquine-treated and untreated cells. Images are representative from 2 unique donors.

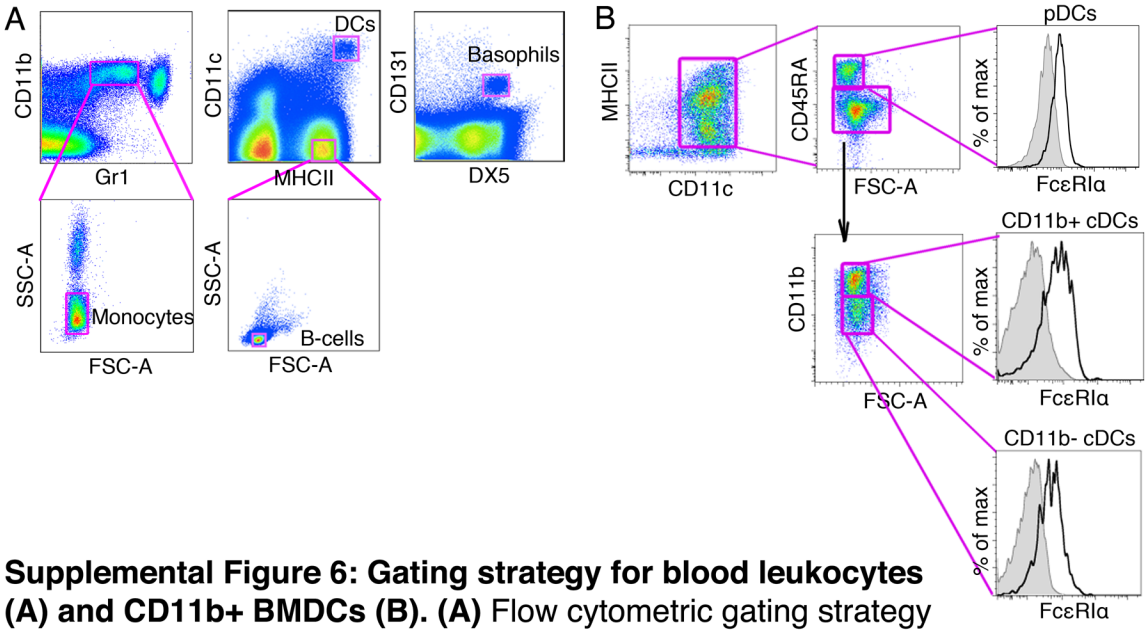

Supplemental Figure 6: Gating strategy for blood leukocytes (A) and CD11b+ BMDCs (B). (A) Flow cytometric gating strategy used for the experiment described in Figure 4A. **(B)** Bone marrows were isolated from hFcεRIα-Tg mice and cultured for 6 days in the presence of 100 ng/mL Flt3L. Generated cells were stained using a cocktail of antibodies and each DC subset was gated as shown. Expression of FcεRI (Black) was also determined compared to isotype control (grey).

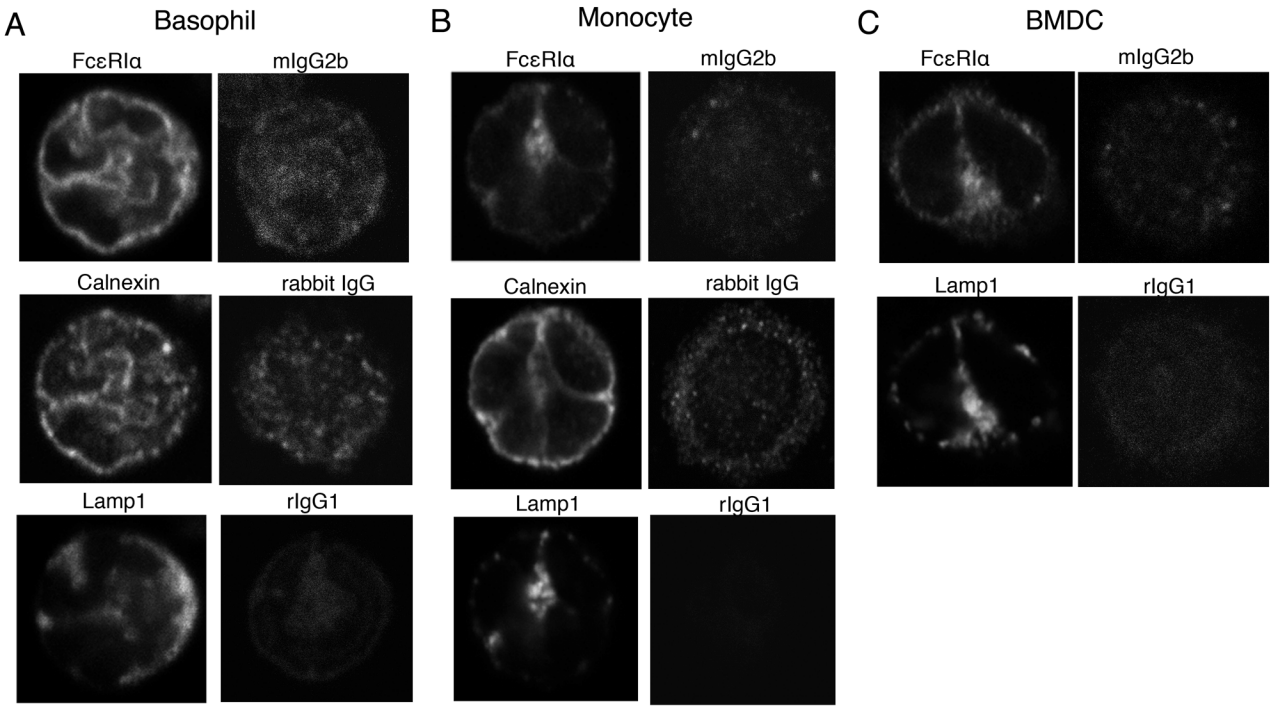

Supplemental Figure 7: Isotype controls for confocal microscopy of mouse blood cells and BMDCs. Blood Basophils **(A)**, monocytes **(B)**, and CD11b+ Flt3L-derived BMDCs **(C)** were isolated as described in methods and were stained with antibodies indicated (left columns) or with the corresponding isotype controls (right columns). Images were taken with the same laser intensity and gain for the antibodies indicated compared to isotype controls.

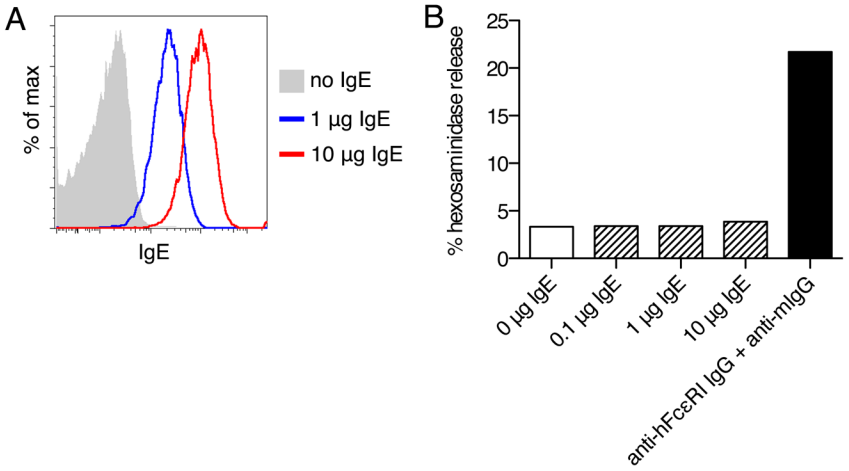

Supplemental Figure 8: Purified human IgE (Abcam) does not degranulate hFcεRI-expressing bone-marrow derived mast cells (BMMCs). BMMCs cultured from hFcεRIα-transgenic mice were incubated with varying concentrations of human IgE (Abcam) or anti-hFcεRI IgG/ anti-mouse IgG Ab complex. **(A)** Binding of IgE was determined by flow cytometry. **(B)** Degranulation was determined by hexosaminidase assay.

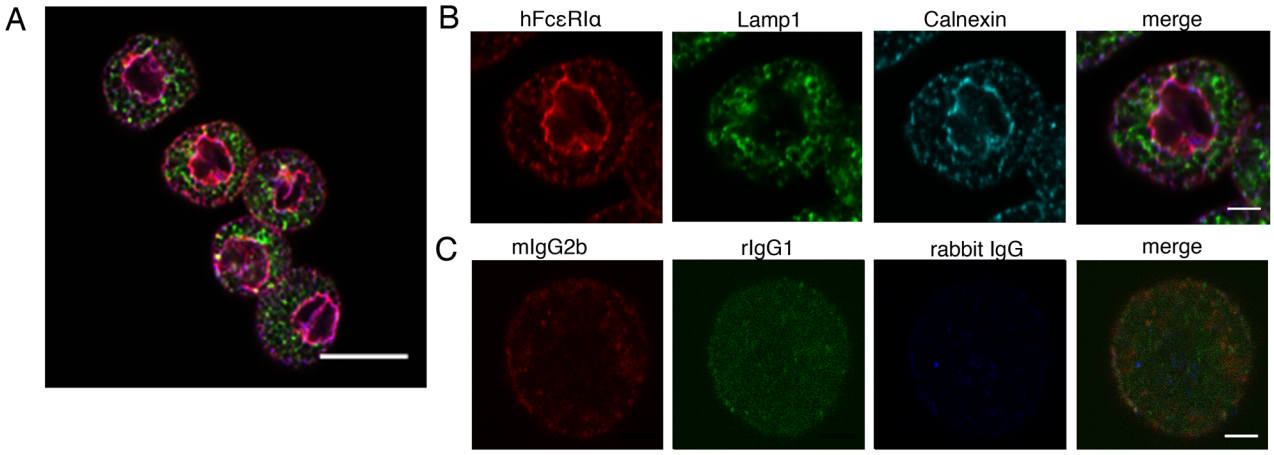

Supplemental Figure 9: hFcεRIα in peritoneal mast cells of hFcεRI-Tg mice is located in the ER, not in the lysosome. Peritoneal mast cells were isolated from peritoneal lavage cells of hFcεRIα-transgenic mice by flow-cytometric sorting based on expression of c-kit and side-scatter properties. Sorted cells were placed on coverslips and stained as described in methods for hFcεRIα, Lamp1, and calnexin, then imaged by confocal microscopy at 60x. **(A)** A group of mast cells. hFcεRIα is in red, Lamp1 is in green, and Calnexin is in blue. Size bar is 10 µm. **(B)** One mast cell imaged at higher magnification. Note that Calnexin is changed to cyan in single-color format for ease of visualization. Size bar is 2.5 µm. **(C)** Isotype controls for stains shown in (B). Images were taken with the same laser intensity and gain for the antibodies indicated compared to isotype controls.

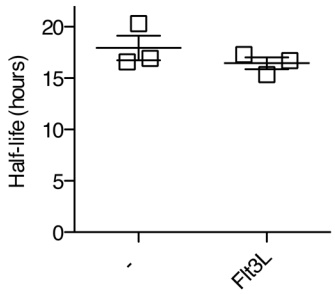

Supplemental Figure 10: Flt3L does not accelerate serum hIgE clearance in Tg$^-$ mice. Half-lives of human IgE in Tg$^-$ mice or Tg$^-$ mice implanted with Flt3L-transfected B16 melanomas. Half-lives are not significantly different as measured by Student's T-test.

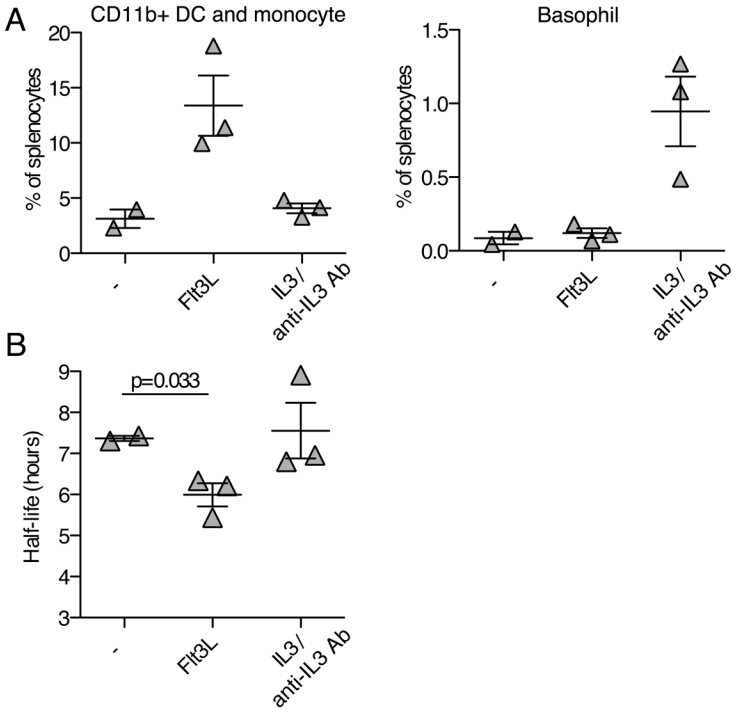

Supplemental Figure 11: Flt3L, but not IL-3, accelerates serum IgE clearance in 10:90 (Tg^+:Tg^-) mixed chimeric mice. (A) The percentage of [CD11b+ DCs + monocytes] or basophils in spleen was determined by flow cytometry. Data are plotted as mean ± SEM. **(B)** Serum human IgE half-lives were determined as described in Figure 6. Significance was determined by Student's T-test.